



Table 2-1-4 Interconnected National Grid (SNI): Installed Capacity (as December 2000)

国内電力供給網(SNI)率下の設備容量

No	PLANTS	UNITS	CAPACITY		COMMISSION DATE	LOCATION		OWNER
			INSTALLED MW	FIRM MW		MUNICIPALITY	DEPARTMENT	
	<b>NATIONAL GRID</b>		<b>1666.3</b>	<b>1420.0</b>				
	<b>HYDROELECTRIC</b>		<b>528.90</b>	<b>477.00</b>				
1	CHIXOY	5	300.00	275.0	1983/11/27	San Cristobal	Alta Verapaz	INDE
2	AGUACAPA	3	90.0	75.0	1981/2/22	Pueblo Nuevo	Santa Rosa	INDE
3	JURUN MARINALA	3	60.0	60.0	1970/2/12	Palin	Escuintla	INDE
11	SECACAO	1	15.5	13.5	1998/7/3	Senaha	Alta Verapaz	PRIVATE
4	ESCLAVOS	2	14.0	13.5	1966/8/17	Cuilapa	Santa Rosa	INDE
15	PASABIEN	2	12.0	12.0	2000/6/6	Rio Hondo	Zacapa	PRIVATE
10	RIO BOBOS	1	10.0	10.0	1995/8/10	Quebradas, Mo	Izabal	PRIVATE
16	POZA VERDE	2	8.1	8.0	2000/1/18	Pueblo Nuevo	Santa Rosa	PRIVATE
	<b>MICHATOYAS</b>	5	6.7	1.5	2027/10/15	Escuintla	Escuintla	INDE
5	SANTA MARIA	3	6.0	6.0	1966/6/25	Zunil	Quetzaltenango	INDE
	EL JOCOTE (Cogenerador)	1	4.0	0.0	1991/2/4	Siquinala	Escuintla	PRIVATE
6	EL PORVENIR	1	2.0	2.0	1968/9/1	San Pablo	San Marcos	INDE
	CHICHAIC	2	0.6	0.5	1979/7/26	Coban	Alta Verapaz	INDE
	<b>THERMAL</b>		<b>1137.4</b>	<b>943.0</b>				
	<b>STEAM TURBINES</b>		<b>221.0</b>	<b>177.0</b>				
18	SAN JOSE	1	142.0	120.0	2000/1/1	Masagua	Escuintla	PRIVATE
7	ESCUINTLA VAPOR 2	1	53.0	35.0	1977/4/22	Escuintla	Escuintla	INDE
7	GGG VAPOR 3	1	13.0	11.0	1959/12/3	Amatitlan	Guatemala	PRIVATE
7	GGG VAPOR 4	1	13.0	11.0	1961/4/5	Amatitlan	Guatemala	PRIVATE
	<b>GAS TURBINES</b>		<b>391.5</b>	<b>293</b>				
19	TAMPA	2	80.0	78.0	1995/12/1	Escuintla	Escuintla	PRIVATE
7	GGG STEWART & STEVENSON	1	51.0	24.0	1994/12/24	Escuintla	Escuintla	PRIVATE
7	ESC. GAS 5	1	41.0	30.0	1985/11/1	Escuintla	Escuintla	INDE
7	GGG GAS 4	1	33.0	27.0	1963/6/11	Amatitlan	Guatemala	PRIVATE
7	ESC. GAS 3	1	25.0	21.0	1976/8/9	Escuintla	Escuintla	INDE
7	ESC. GAS 4	1	25.0	*	1976/8/9	Escuintla	Escuintla	INDE
7	GGG GAS 2	1	23.0	17.0	1978/6/19	Amatitlan	Guatemala	PRIVATE
7	ESC. GAS 2	2	12.5	*	1968/5/7	Escuintla	Escuintla	INDE
7	GGG GAS 1	1	11.0	6.0	1964/6/6	Amatitlan	Guatemala	PRIVATE
	<b>INTERNAL COMUSTION ENGINES</b>		<b>422.2</b>	<b>375.8</b>				
17	LA ESPERANZA(ENRON POWER 3)	7	126.0	124.0	2000/5/1	Puerto Quetzal	Escuintla	PRIVATE
17	PQPC (ENRON POWER)	20	110.0	102.5	1993/2/5	Puerto Quetzal	Escuintla	PRIVATE
7	GGG LAS PALMAS	5	66.8	65.0	1998/9/1	Escuintla	Escuintla	PRIVATE
20	SIDEGUA	10	44.0	36.0	1995/4/3	Escuintla	Escuintla	PRIVATE
14	GENOR	2	42.4	40.0	1998/10/1	Puerto Barrios	Izabal	PRIVATE
	CEMENTOS PROGRESO (Autoproductor)	1	18.0	3.3	1995/11/16	Sanarate	El Progreso	PRIVATE
13	LAGOTEX	3	15.0	5.0	1996/11/15	Amatitlan	Guatemala	PRIVATE
17	PQPC (ENRON POWER)	20	120.0	102.5	2000/2/5	Puerto Quetzal	Escuintla	PRIVATE
	<b>SUGGAR MILLS (Cogenerators)</b>		<b>163.7</b>	<b>163.7</b>	<b>1996/12/31</b>	<b>Varios</b>	<b>Escuintla</b>	<b>PRIVATE</b>
25	PANTALEON		38.5	38.5	1995/11/16		Escuintla	PRIVATE
23	SANTA ANA		33.8	33.8	1996/11/16		Escuintla	PRIVATE
27	LA UNION		29.5	29.5	1997/11/16		Escuintla	PRIVATE
22	CONCEPCION	1	27.5	27.5	1998/11/16		Escuintla	PRIVATE
26	MADRE TIERRA		19	19	1999/11/16		Escuintla	PRIVATE
24	MAGDALENA		15.4	15.4	2000/11/16		Escuintla	PRIVATE
	<b>GEOTHERMAL</b>		<b>29</b>	<b>23.5</b>				
9	ZUNIL	1	24	19	1999/8/4	Zunil	Quetzaltenango	PRIVATE
8	CALDERAS	1	5	4.5	1998/11/1	San Vicente Pa	Escuintla	PRIVATE

Source: Genetec

**Table 2-1-5 Present coverage and growth rate of electrification  
per Department (県別電気利用者数とその上昇率)**

Department	Customers	Coverage	1991-2000
			Increment
Guatemala	514,463	94.8	6.3
Solola	48,914	93.9	51.1
Sacatepequez	42,640	91.3	18.0
Quetzaltenango	101,762	91.2	42.2
Totonicapan	57,882	90.8	44.5
Santa Rosa	54,986	90.5	45.9
Chimaltenango	66,987	89.7	44.6
El progreso	24,507	86.5	34.3
Zacapa	33,853	85.9	32.7
Retalhuleu	36,411	83.3	56.8
Escuintla	73,853	79.5	33.8
Suchitepequez	50,035	70.8	33.4
San Marcos	94,488	66.4	46.5
Jutiapa	48,838	65.8	27.1
Izabal	36,776	62.0	34.9
Baja Verapaz	23,655	61.3	38.6
Huehuetenango	88,501	60.9	45.6
Jalapa	25,534	59.1	28.6
Chiquimula	31,937	58.4	20.4
Quiche	60,656	54.8	40.9
Peten	25,108	47.3	30.6
Alta Verapaz	33,337	29.3	18.5
Total	1,575,123	76.4	32.0

Source: MEM

全国電気卸売事業会による電力需要予測

<b>Year</b>	<b>Generation</b>	<b>% Growth</b>	<b>Capacity</b>	<b>% Growth</b>	<b>Load Factor</b>
	<b>GWH</b>		<b>MW</b>		<b>p.u.</b>
1999	4885.1	8.98%	962	9.77%	0.580
2000	5348.2	9.48%	1048	8.88%	0.583
2001	5805.9	8.56%	1133	8.20%	0.585
2002	6294.4	8.41%	1229	8.41%	0.585
2003	6809.1	8.18%	1317	7.20%	0.590
2004	7347.2	7.90%	1403	6.50%	0.598
2005	7929.1	7.92%	1494	6.50%	0.606
2006	8492.6	7.11%	1578	5.60%	0.615
2007	8978.9	5.73%	1666	5.60%	0.615
2008	9485.1	5.64%	1759	5.60%	0.615
2009	9995.8	5.38%	1859	5.64%	0.614
2010	10495.6	5.00%	1957	5.30%	0.612
2011	11020.4	5.00%	2051	4.80%	0.613
2012	11571.4	5.00%	2149	4.80%	0.615
2013	12150.0	5.00%	2253	4.80%	0.616
2014	12757.5	5.00%	2361	4.80%	0.607
2015	13395.3	5.00%	2474	4.80%	0.618

Source [www.amm.org.gt](http://www.amm.org.gt)

釧山エネルギー省による電力需要予測  
**Table 2-1-7 Interconnected Grid (SNI): Scenarios for Energy Demand Forecast**

Year	Medium				High				Low			
	Capacity (MW)	Energy (GWh)	Annual Growth (%)	Capacity	Energy (GWh)	Annual Growth (%)	Capacity	Energy (GWh)	Annual Growth (%)	Capacity	Energy (GWh)	Annual Growth (%)
			Capacity	Energy	Capacity	Energy	Capacity	Energy	Capacity	Energy	Capacity	Energy
2000	1,049	5,348		1,049	5,348		1,049	5,348		1,049	5,348	
2001	1,137	5,819	8.4	1,160	6,035	10.6	1,123	5,760	7.1	1,199	6,189	7.5
2002	1,231	6,319	8.3	1,270	6,620	9.5	1,275	6,672	8.9	1,350	7,159	7.3
2003	1,322	6,812	7.4	1,379	7,207	8.6	1,423	7,574	7.9	1,495	7,982	5.4
2004	1,414	7,309	7.0	1,490	7,809	8.1	1,567	8,387	7.2	1,636	8,807	4.4
2005	1,505	7,806	6.4	1,603	8,425	7.6	1,705	9,243	6.7	1,775	9,674	4.1
2006	1,596	8,306	6.1	1,717	9,051	7.1	1,836	9,704	6.9	1,954	10,382	6.0
2007	1,689	8,821	5.8	1,836	9,704	6.2	2,079	11,077	6.4	2,206	11,774	6.1
2008	1,779	9,350	5.3	1,954	11,382	6.4	2,079	11,077	6.4	2,206	11,774	6.1
2009	1,874	9,883	5.3	2,079	11,077	6.4	2,206	11,774	6.1	2,206	11,774	6.1
2010	1,967	10,407	5.0	2,206	11,774	6.3						

Source MEM

Table 2-1-8 Country Over view  
 グアテマラ国の一般概況

Item	Fact
President:	Alfonso Portillo (since January 2000)
Independence:	September 15, 1821 (from Spain)
Population (2000E):	12.6 million
Location/Size:	Central America, bordering the Pacific Ocean between Belize, El Salvador, Honduras, and Mexico/42,042 square miles
Capital:	Guatemala City
Languages:	Spanish (official), Mayan languages
Ethnic Groups:	Mestizo 56%, Amerindian 44%
Religion:	Roman Catholic, Protestant, Mayan
Defense:	(8/98) 31,400 (29,200 Army, 1,500 Navy, 700 Air Force)

Source: Energy International association, DOE

**Table 2-1-9 Economic Overview**  
**グアテマラ国の経済指標**

Item	Fact
Minister of Economy:	Raul Edmindo Archilla Serrano
Currency:	Quetzal
Market Exchange Rate (3/23/01):	1 US Dollar = 7.68 Quetzals
Gross Domestic Product (GDP, nominal, 1999E):	\$17.8 billion (2000E): 19.0 billion
Real GDP Growth Rate (2000E):	3% (2001F): 2.7%
Inflation Rate (consumer prices, 2000):	6% (2001F): 5%-10%
Trade Deficit (2000E):	\$2.1 billion
Current Account Deficit (2000E):	\$1 billion
External Debt (2000E):	\$2.5 billion
Major Trading Partners:	United States, El Salvador, Mexico, Germany, Japan
Major Export Products:	coffee, sugar, bananas
Major Import Products:	Non-durable goods, industrial raw materials and intermediate goods, capital goods

Source: Energy International association, DOE

**Table 2-1-10 Environmental Overview**  
**グアテマラ国の環境的指標**

<b>Item</b>	<b>Fact</b>
Total Energy Consumption (1999E):	0.15 quadrillion Btu*(<0.1% of world total energy consumption)
Energy-Related Carbon Emissions (1999E):	2.4 million metric tons of carbon(<0.1% of world carbon emissions)
Per Capita Energy Consumption (1999E):	12.3 million Btu (vs. U.S. value of 355.8 million Btu)
Per Capita Carbon Emissions (1999E):	0.2 metric tons of carbon (vs. U.S. value of 5.5 metric tons of carbon)
Energy Intensity (1999E):	13,181 Btu/\$1990 (vs. U.S. value of 12,638 Btu/\$1990)**
Carbon Intensity (1999E):	0.22 metric tons of carbon/thousand \$1990 (vs. U.S. value of 0.19 metric tons/thousand \$1990)
Sectoral Share of Energy Consumption (1998E):	Residential (49.1%), Industrial (22.6%), Transportation (21.1%), Commercial (7.2%)
Sectoral Share of Carbon Emissions (1998E):	Transportation (48.3%), Industrial (35.3%), Residential (9.8%), Commercial (6.6%)
Fuel Share of Energy Consumption (1999E):	Oil (84.9%), Natural Gas (0.0%), Coal (0.0%)
Fuel Share of Carbon Emissions (1999E):	Oil (100.0%), Natural Gas (0.0%), Coal (0.0%)
Renewable Energy Consumption (1998E):	160 trillion Btu* (2% decrease from 1997)
Number of People per Motor Vehicle (1998):	58.8 (vs. U.S. value of 1.3)
Status in Climate Change Negotiations:	Non-Annex I country under the United Nations Framework Convention on Climate Change (ratified December 15th, 1995). Guatemala has ratified the Kyoto Protocol (October 5th, 1999).
Major Environmental Issues:	Deforestation; soil erosion; water pollution; Hurricane Mitch damage. Major International Environmental Agreements: A party to the Antarctic Treaty, Biodiversity, Climate Change, Desertification, Endangered Species, Environmental Modification, Hazardous Wastes, Law of the Sea, Marine Dumping, Nuclear Test Ban, Ozone Layer Protection, Ship Pollution and Wetlands. Has signed, but not ratified, the Antarctic-Environmental Protocol.

Source: Energy International association, DOE

\* The total energy consumption statistic includes petroleum, dry natural gas, coal, net hydro, nuclear, geothermal, solar and wind electric power. The renewable energy consumption statistic is based on International Energy Agency (IEA) data and includes hydropower, solar, wind, wood, waste electrical power, tide, geothermal, solid biomass and animal products, biomass gas and liquids, industrial and municipal wastes. Sectoral shares of energy consumption and carbon emissions are also based on IEA data.

\*\*GDP based on EIA International Energy Annual 1999



## 2.2 Geoscientific Studies

2.2.1 Geological Survey

2.2.2 Geochemical Survey

2.2.3 Gravity Survey

2.2.4 Magnetotelluric Survey



## 2.2 GEOSCIENTIFIC STUDIES

### 2.2.1 Geological Survey

The purpose of this geological survey was to grasp the geology and structure controlling the geothermal activity through the geological reconnaissance, rock sampling and review of the existing report. The analysis was conducted by the understanding of the distribution of young volcanic bodies, alteration zones and their characteristics, heat sources and hydrogeology in the study area and its surroundings.

The field survey consists of geological mapping, structural and fractures studies and mapping of alteration zones. The laboratory services included microscopic observation (13 samples), X-ray analysis (Bulk 25 samples and Clay 20 samples), zircon crystal morphology (10 samples), zircon Fission Track (FT) dating (5 samples) and Thermo-Luminescence (TL) dating (volcanic dating of 5 samples and alteration dating 5 samples) on samples collected during the field survey.

Based on the interpretation of the volcanic transition and on the hydrothermal alteration, the history of the geothermal activity was reconstructed and its relation to the geothermal structure was estimated.

#### 1. Regional Geology

Guatemala is located in the northern portion of Central America, between the North American Continent and the South American Continent, bounded by Mexico on the north and Honduras-El Salvador at the south, and facing the Pacific Ocean at its southwestern side and the Caribbean Sea at its northeastern side. The Amatitlan area, which is the target area of this project, is located on the northern flank of the Pacaya volcano, 25 km far to the south from Guatemala City (Fig. 2-2-2).

This mountain range at the altitude between 1,200-2,000masl is the site for several volcanoes active in the last 100 years; Pacaya (at the south of the surveyed area), Acatenango, Santa Maria, and Santiagito all aligned in a NW-SE direction. The chain of volcanoes is called the Central American Volcanic Arc with the constant separation from each other starts from the Tacana volcano (at the border between Mexico and Guatemala) to the Irazu volcano in the central Costa Rica.

As illustrated in Fig. 2-2-1, the Mid-American Trench, with axis in NW-SE direction, is located at 100km southwest of the Guatemalan seashore. This trench is considered to be a boundary between the subducting Cocos Plate (subducting from the SW) and Caribbean Plate (Molnar and Sykes, 1969). Subduction of the Cocos Plate is accompanied by a volcanic front (Sugiyama, 1960), which formed the central-American volcanic arc of strike parallel to Mid-American Trench. The volcanic chain in NW-SE direction was formed by the NE-SW trending extensional stress field caused by an active uplift along the southwestern margin of Caribbean Plate, which in turn resulted from the subduction of Cocos Plate in a N30°E direction.

#### 2. Geology at the Amatitlan Area

The geology of this area consists of granitic basement rock, pre-caldera, syn-

caldera and post-caldera volcanic rock formation, (including the Amatitlan volcanic complex consisted from dominant pyroxene andesite and subdominant dacite), the Pacaya volcanic complex and alluvium and colluvium (Fig. 2-2-3 and Fig. 2-2-4).

The geological features of the Amatitlan area are represented by caldera related faults, N-S and NE-SW faulting, and emplacement of dacitic dome. Along these structures trending, hot springs and fumaroles are located and the surface altered areas are elongated.

Their structures and their relation to geothermal manifestations are described as follows.

a. Caldera structure

The results of drilling deep exploratory wells AMF-1, -3 and -4 (West JEC and Telectro, 1995) revealed an E-W system of faults near Laguna caldera. This fault was associated to the south edge of the caldera. The geothermal fluid might be finding easy flow path through this fault system. However, the shallow portion of these faults is likely to be an inflow area of shallow ground water meaning the presence of recharge zone at this south rim of the caldera covered thickly with volcanics from the Amatitlan volcanic complex (Fig. 2-2-5).

On the other hand, many fumaroles and alteration zones are present at the north wall of the Laguna caldera. The arrangement of alteration zones and fumaroles is parallel to the western discontinuity direction interpreted from the results of gravity and MT investigations.

At Los Humitos, fumaroles are located apparently close to the fault of the eastern edge. Since this caldera is supposed to have been formed by a steam explosion, it is very possible that the caldera edge is a subsidence caused by a fault.

b. Principal fault system

The N-S fault setting is found developed in parallel direction at both sides of Los Humitos caldera. The post caldera volcanics are found altered at the west side of the western fault bounding this N-S fault system. This suggests a young geothermal activity. The west end of Los Humitos caldera has been argillized to up to a certain depth, forming a sealing zone. While the east side of the caldera shows a poor progress in alteration, suggesting a still present open fracture zone.

c. Dacitic domes

It is presumed that hot springs and fumaroles of Lake Amatitlan are originated in a fracture zone developed around the dacitic domes. However, few hot spring and fumaroles could be recognized along the fracture associated to the N-S fault system. Therefore, the fracture zone was developed at the boundary between the dome and the surrounding materials when the dacitic magma rose to form the dome. This fracture very possibly represents a path for geothermal fluid to flow. Furthermore, it is possible that this dacite dome itself is one of the heat sources in this area, considering fluid geochemistry and the formation time of the dome.

### 3. Heat sources

It is clear that the center of the volcanic activities have migrated from north to south during the geological history of the Amatitlan area from the distribution of each volcanic rock and the dating results. The hydrothermal activity is also believed to migrate in the same direction. The heat source for the geothermal activities in Amatitlan area is associated to the dacitic magmatism, including that of the still active Pacaya Volcano or to magmatic gases intrusion. This activity spans from the late Pleistocene, approximately 0.7Ma, to present. The geothermal reservoir beneath Laguna Caldera is thought to be associated to an intrusion of magmatic fluids from Pacaya Volcano. However, there is no precise knowledge of the location of the magma reservoir.

West JEC-Telectro (1995) investigated on the heat source using data from the existing data. Following a description of their finding is given.

- a. Among the previous exploratory wells, the site AMF-2 shows the highest temperature. With in the area, a temperature above 300° C was estimated at the top of the basement consisting of granite porphyry.
- b. From the observation of the drilled cuttings and their zircon crystal forms, the similar dacite as a dome-volcano at Los Humitos was found at depth of 560-870 m in Well AMF-2. The radiometric age determination showed the almost same age of some 6,000 years ago.
- c. The homogenization temperature of fluid inclusion from Well AMF-2 shows a bimodal distribution, in which the higher peak coincides with the temperature measured in the well. This may indicate that pre-existing geothermal system was heated up by about 50° C due to the new dacite intrusion. The phenomenon of a bimodal distribution cannot be found in Wells AMF-1, AMF-3 and AMF-4 distant from the dacite intrusion. Therefore, the surrounding area to well AMF-2 may be still heating up by the dacitic intrusion.
- d. In conclusion, dacitic magma's intrusion probably occurred close to Well AMF-2 some 6,000 years ago and could shape the dacitic dome body such as Cerro Limon and El Durazno acts as local heat sources.

### 4. Hydrogeology

The flow pattern of the regional hydrological system controlling that of the Amatitlan area shows a movement toward the south through the Guatemala graven until it reaches the Amatitlan Caldera. The system drains to the Pacific Ocean through the Palin-Michatoya canyon at the west and northwest of the study area. Within the study area, the shallow hydrological flow pattern is from south, Pacaya volcano and Cerro Grande, towards the Amatitlan Lake.

This flow of shallow underground water apparently travels through zones dominated by fractured volcanic lava flow. Since most of the pyroclastic found in the area are loose and highly permeable, the contact of this strata and the underlying materials might become also a good pathway to the flow of this underground water. These porous pyroclastic sediments may become the zone of flow and reservoir of geothermal fluid but in most of the cases, they

are likely to be affected by argillization and silicification making them impermeable to the flow of fluid. In general, fractured zones are related to highly permeable deep faults. Especially, rocks such as volcanic lava, intrusive rocks, basement rocks, etc., are remarkably brittle, making them prone to fracture and then, making them a preferable pathway to the flow of fluids. Accordingly, the target for the surface exploration was to detect fault zones in the study area. However, faults themselves are likely to undergo argillization and to become the impermeable barrier in the direction orthogonal to the fault plane. This explains the common fact found during drilling of recording higher static pressure prior tapping a fault bearing geothermal fluids.

The shallow groundwater in the study area flows from relatively high altitude zone at the north foot of the Pacaya volcano towards the Amatitlan Lake. The underground water infiltrates through the contact between the lava of the Pacaya Combined Volcano - Amatitlan volcanic complex and the pyroclastic rocks derived from the Amatitlan volcanic complex itself.

The rim of the caldera, with center at the Amatitlan lake, is conformed by normal faults. These faults are covered by thick layers of volcanic rocks derived from the activity of the Pacaya and Amatitlan volcanic complex. These faults are not inherent to the flow of the shallow underground water, but might possibly be the passage for the water to penetrate into the deeper zone. Meanwhile in the deeper parts of the system, the geothermal fluid around the faults might be easily channeled in the E-W direction but thinking on the reduced permeability orthogonal to the fault plane, the flow might be restricted in N-S direction. In the neighborhood of the area between Los Humitos Caldera to Laguna Caldera, small-scale N-W trending faults were detected. The geothermal fluids are considered to flow along the faults. These faults are clearly recognized from topographic features and it seems highly plausible that restricted to this area only both, the shallow groundwater and the deep geothermal fluid utilize the same route to flow in N-S direction. This N-S lateral flow was identified when interpreting the temperature profiles recorded at well AMF-3.

### **2.2.2 Geochemical survey**

The geochemical survey aimed to obtain information about the geothermal fluid in the survey area for selecting the sites of exploration well drilling and for planning the future geothermal development. In order to ascertain the geochemical model constructed by the results of the previous geochemical survey, supplemental sampling and analysis of hot spring waters and fumarole gases and review of the existing geochemical information was carried out. Mercury and Radon soil-gas survey was conducted for taking information about distribution of the thermal fluid in the area with no surface manifestations or wells.

#### **1. Hydrogeochemical survey**

##### **a. Survey method**

In order to evaluate the existing chemical data and to obtain additional

isotope data, sulfur and carbon isotope, supplemental sampling and analysis of hot spring waters (6 samples), surface waters (6 samples), and fumarolic and/or bubbling gases (3 samples) in and around the survey area were conducted. Chemical and isotope analyses were carried out in Japan. Locations of surface manifestations and wells, where fluid samples were collected by the field work, are shown in Fig. 2-2-6.

Chemical and isotopic analyses as followings of the water and gas samples collected in the field was carried out.

- ① Hot water: TSM, Na, K, Li, Ca, Mg, Fe, Al, Cl, SO<sub>4</sub>, T-CO<sub>2</sub>, HCO<sub>3</sub>, F, B, Br, I, As, T-SiO<sub>2</sub>, Sr, H<sub>2</sub>S, Hg,  $\delta$  D(H<sub>2</sub>O),  $\delta$  <sup>18</sup>O(H<sub>2</sub>O),  $\delta$  <sup>18</sup>O(SO<sub>4</sub>),  $\delta$  <sup>34</sup>S(SO<sub>4</sub>),  $\delta$  <sup>13</sup>C(HCO<sub>3</sub>), Tr
- ② Surface water: TSM,  $\delta$  D(H<sub>2</sub>O),  $\delta$  <sup>18</sup>O(H<sub>2</sub>O), Tr
- ③ Gas: N<sub>2</sub>, H<sub>2</sub>, CH<sub>4</sub>, C<sub>2</sub>H<sub>6</sub>, O<sub>2</sub>, Ar, He, Ne, <sup>3</sup>He/<sup>4</sup>He, <sup>4</sup>He/<sup>20</sup>Ne,  $\delta$  <sup>13</sup>C(CO<sub>2</sub>),  $\delta$  <sup>13</sup>C(CH<sub>4</sub>),  $\delta$  D(H<sub>2</sub>),  $\delta$  D(CH<sub>4</sub>),  $\delta$  <sup>34</sup>S(H<sub>2</sub>S)

#### b. Results of interpretation

The characteristics and behaviors of hydrothermal systems in and around the survey area, inferred from the results of geochemical interpretation by this survey, are summarized as follows. The geochemical model of hydrothermal system based on the interpretation is shown in Fig. 2-2-7.

- The hot water of the reservoirs confirmed by the deep exploration wells AMF-1 and AMF-2 in Calderas sector is considered to be derived from the hot parental of 300-340°C originating from meteoric water with minor magmatic fluid, which is stored at the south of the well AMF-2. The hot water in this sector flows mainly northeastward with steam separation, and partly ascends to shallower level producing the fumarolic fluids.
- The hot water from Calderas flows laterally toward north and northeast directions with dilution by cool groundwater, and finally reaches the south shore of Lago de Amatitlán, providing the Cl or Cl-HCO<sub>3</sub> type hot spring aquifers. The hot water reaching the lake shore at the northwest of the slim hole AM-1 is probably re-heated at the area near the lake shore. The maximum temperatures of the hot water near the lake shore are estimated 250°C at the deeper level and 200°C at the shallower level respectively.
- The hot water from Calderas also reaches the east edge of Río Michatoya valley. The outflow of the hot water is thought to be relatively rapid, though strongly diluted. The hot water expands around in the area of Río Michatoya S and NE and is mixed with shallow groundwater, forming the Cl-HCO<sub>3</sub> or HCO<sub>3</sub> type hot spring aquifers with maximum temperature of ca.140°C.
- Another hot fluid system, besides that of Calderas, is present in an area of around the slim hole AM-5. The hot water in this system originates in meteoric water mainly from the northwest side, and is relatively poor in

Cl. The water temperature at deeper level is estimated at ca.210°C. The hot water spreads at the shallow level in the area of Río Michatoya NW.

- The hot water reservoir in Calderas is considered to have some extents in its scale, since the water seems to be in chemical equilibrium at the reservoir. If a permeable zone(s) exists from around the well AMF-2 toward the west in the survey area, the hot water reservoir may extend along that zone(s).

## 2. Soil-gas survey

### a. Survey method

Mercury and radon gas concentration in the soil-gas were measured at the field in and around the survey area. The distributions of anomaly zone were clarified with statistic analyses and making contour maps. The results of soil-gas survey were interpreted with considering the information by the fluid geochemical survey.

For measurement of Hg and Rn concentration in soil-gas, two sampling holes (5cm diameter, 60cm depth) were made for individual component at each sampling station. Mercury was measured by a portable Hg detector (PM-1A; Nippon Instruments Co.), and radon was measured by a portable Rn detector (RD-200; EDA Instruments Inc.).

### b. Results of interpretation

From the distribution of Hg and total-Rn concentration in soil-gas, the area of hot fluid up-welling and the sub-surface structure controlling the hot fluid in the survey area are inferred as follows. The compiled map of permeable zone by soil-gas survey is shown in Fig. 2-2-8.

- Along the north caldera wall of Calderas, a permeable zone exists accompanied by hydrothermal activity; and hot fluids ascend to the shallow level at the western Calderas and around Cerro Hoja de Queso. The permeable zone in the western Calderas elongates NE-SW direction, reaching the south of El Cedro and suggesting that the geothermal reservoir confirmed by the well AMF-1 and AMF-2 extends to southwest.
- The extending direction of the moderately high Hg area around El Cedro elongating to northwest appears to have a relation with the outflow of hot water from Calderas to Río Michatoya valley which is inferred from the result of the fluid-geochemical survey.
- Permeable zones exist from around Cerro Hoja de Queso to the northwest and north, where hot fluids flow laterally at the shallow level. In this area, the hydrothermal activities decline at the northwest and north parts, and the direct up-welling of hot fluids from the deeper level is not expected.
- From the north of Cerro Hoja de Queso to the west of Cerro Grande, a permeable zone exists showing N-S and NE-SW trends. Although hydrothermal activity along this zone is not ascertained, there is a possibility that deep hot fluids heated around Cerro Grande and/or



Volcán de Pacaya flow to the north.

### 2.2.3 Gravity and Magnetic Survey

Gravity and magnetic survey are geophysical prospecting methods useful to disclose the underground geologic structure. This is done by interpreting gravity anomalies caused by variations in the density of the subsurface and by interpreting magnetic anomalies caused by variation in the magnetic properties of underground materials.

#### 1. Contents of survey

204 stations were measured for gravity and magnetic survey. LaCoste G-579 gravity meter manufactured by LaCoste & Romberg, an American manufacturing firm, was used for the gravity measurements. Gravity raw data were generated after applying reading converted to milligals, tidal correction, instrument height correction and drift correction. A G-866 recording proton magnetometer and a G-856 portable proton magnetometer manufactured by EG&G Geometrics, an American manufacturing firm, were used for the magnetic survey. The location and elevation of the stations were determined by a GPS static survey. A 4000ST and a 4600LS GPS receiver manufactured by Trimble, an American manufacturing firm, were used.

Bouguer anomalies were calculated by subtracting free-air correction, terrain correction, Bouguer correction and atmosphere correction from gravity raw data. IGRF (*International Geomagnetic Reference Field*) residuals were calculated by subtracting correction of diurnal variations and standard magnetic field correction. Filtered maps and two-dimensional models were drawn from Bouguer anomalies and IGRF residuals.

#### 2. Results of interpretation

##### a. Gravity method

Fig. 2-2-9 shows the results of the gravity. Bouguer anomaly decreases from south to north. Many lineaments which seem to reflect subsurface structures are recognized from the Bouguer anomaly map, residual gravity map, second vertical derivative map and gravity gradient map. These linear features will be called "gravity lineaments" hereafter.

Bouguer anomaly ranges from  $-48.2$  mgal at the north to  $-10.4$  mgal at south of the survey area. The survey area consists of two parts: the northern part corresponds to the Amatitlan low-gravity anomaly area and southern part corresponds to the Volcan de Pacaya high-gravity anomaly area. The Amatitlan low-gravity anomaly area is considered to reflect the caldera structure. Bouguer anomaly contour  $-35$  mgal corresponds to the south end of the caldera rim. According to the results of the gravity section modelling, gravity basement depresses more than 500 m to the north to the caldera rim. Here, it was found that low-density sediments thickly overlay the bottom of the caldera. At the southern caldera rim, the Volcan de Pacaya high-gravity anomaly reflects the basement uplift (namely "Volcan de Pacaya basement uplift" in this report) extending in N-S direction. Well

AMF-1 located over this basement uplift encountered basement granite at an elevation of about 300 masl, showing evidence shallow basement. Gravity basement in this area steps down towards the north with. A basin is estimated south of Laguna de Calderas within this basement uplift.

At both, east and west sides of the extension of the Volcan de Pacaya basement uplift, the Bouguer anomalies change rapidly and it is where gravity lineament was disclosed. The gravity lineament west of the basement uplift extends in N-S direction at the north end and in NE-SW direction from El Pepinal to the southwest of well AMF-2. This gravity lineament departs in two branches from the southwest of well AMF-2 to the southwest and south. That in south direction is clearer than southwest direction. The gravity lineament east of the basement uplift extends in N-S direction at the north of the lineament, in NE-SW direction at the east of Laguna de Calderas, in NW-SE direction at 1.5 km north of Cerro Grande and in N-S direction at the south of this lineament.

A basin 1-km distance across, is recognized at the western side of El Cedro. It is surrounded by a basement uplift so that a buried crater is estimated.

The gravity lineament west of the Volcan de Pacaya basement uplift is considered to reflect a high permeable zone and to be a very promising area for drilling for geothermal developments. Because wells AMF-1, AMF-2 and AMF-3 are locate along this gravity lineament, and this is the reason for wells AMF-1 and AMF-2 to succeed in producing geothermal fluids and for well AMF-3 to show large scale lost of circulation at depth.

#### b. Magnetic method

The Magnetic interpretation map is shown in Fig. 2-2-10. This map shows magnetic discontinuities, which were obtained from the magnetic analysis map. The magnetic anomaly bodies, were obtained from a two-dimensional magnetic model analysis. The followings describe the magnetic structure with consideration to the gravity structure.

In this survey area, the total magnetic intensity field in the survey area ranges from 39,600 nT between the top and the southeast slope of Cerro Grande to 37,800 nT, 1 km east of Laguna de Calderas. Most the magnetic discontinuities are running NE-SW. In the central survey area, low-magnetic anomaly extends N-S, which corresponds in the gravity basement uplift. This low-magnetic anomaly is considered to result from the fact that the susceptibilities of granites are relatively lower than other rocks in this area, and that the upper boundary of granites is relatively shallow. Particularly, low-magnetic anomaly indicates lower values at San Francisco de Sales and Laguna de Calderas, where a gravity basin is estimated and which is considered to be in connection with low density layer near surface. A geothermal alteration is observed near AMF-1. It is considered that the low-magnetic anomaly reflects the decay of magnetic intensity in the low-density layer due to geothermal alteration.

The magnetic discontinuity, locate west of the low-magnetic anomaly at Laguna de Calderas, corresponds with gravity lineaments. This magnetic discontinuity is considered to reflect high permeable zone and to be a very promising area for drilling for geothermal development. Because wells

AMF-1, AMF-2 and AMF-3 are located along this gravity lineament, and this is the reason for wells AMF-1 and AMF-2 to succeed in producing geothermal fluids and for well AMF-3 to show large scale loss of circulation at depth

High-magnetic anomaly extending from north of Cerro Grande to the northeast corresponds to the surface distribution of Pacaya volcanic rocks. Low-magnetic anomaly, 1 km southwest of El Cedro corresponds to the gravity basin where a distribution of low-density and low-magnetic susceptibility layer was found.

#### **2.2.4 Magnetotelluric survey**

The objective of the magnetotelluric (MT) survey with dense station configuration is to delineate promising zones for geothermal development by studying the detailed subsurface resistivity distribution derived from the magnetotelluric survey results. In particular, delineating the locations of the fracture systems, which usually indicate resistivity discontinuities, around the AMF-1 well, AMF-2 well and the caldera wall and delineating the cap rock zones, which usually indicate low resistivity zones, are important in selecting future drilling targets.

### **3. Contents of the survey**

Survey method : Remote-reference Magnetotelluric survey

Survey area : Approximately 21km<sup>2</sup>

Number of measured stations : 61 stations

Acquired electromagnetic signals :

3 components of magnetic signal (H<sub>x</sub>, H<sub>y</sub>, H<sub>z</sub>)

2 components of electric signal (E<sub>x</sub>, E<sub>y</sub>)

Frequencies : 384Hz ~ 0.00055Hz

( Apparent resistivity value and phase values at 40 frequencies which range from 384Hz to 0.00055Hz were calculated. )

### **4. Resistivity Discontinuities**

The resistivity discontinuity is a structure which exhibits a big change in resistivity and/or apparent resistivity laterally. If such structures are distributed continuously along a line, a fault system and/or fracture system is expected to be located along these discontinuity structures. In general, geothermal fluid is trapped in and around the fault/fracture system, so detecting the resistivity discontinuities is important in studying the geothermal structure in the survey area. In the Amatitlan survey area, the resistivity discontinuities F1, F2, F3, F4, and F5 are recognized based on the survey results.

The resistivity discontinuities location map is shown in Fig.2-2-11.

#### **a. Resistivity Discontinuity F1**

Resistivity discontinuity F1 runs from the area beside station 40 to the area beside station 7 passing along the southern end of Laguna de Calderas roughly in a ENE-WSW direction.

The northeast portion of discontinuity F1 is recognized only in the depth map of the top of the resistivity basement and the resistivity map for a depth of 500m, however the discontinuity is not recognized in the resistivity map for a depth of 1500m and that for 3000m which show the deep resistivity structure. Therefore, the northeast portion of F1 probably exist only at shallow depths but not at deep depths.

On the other hand, since the southwest portion of the resistivity discontinuity F1 is recognized in the resistivity map for a depth of 1500m and 3000m and the resistivity section maps (section ① ~ ⑥), the southwest portion of F1 probably reflects a fracture system developed in the deep zone.

The uplifted structure of the resistive zone at depth is clearly recognized along and to the north of discontinuity F1. And the low resistivity zone which probably reflects a hydrothermally altered zone is clearly recognized on the resistive zone at depth. Therefore, F1 is considered to be a fracture system which controls geothermal fluid at depth.

#### b. Resistivity Discontinuity F2

Resistivity discontinuity F2 runs from the north of Cerro Chino to the area between station 9 and 10 roughly in a NNW-SSE direction.

Discontinuity F2 is recognized in the apparent resistivity map (1.125Hz), the resistivity map of low resistivity layers, the depth map of the top of the resistivity basement and the resistivity map for a depth of 500m, but is not recognized on the resistivity maps showing resistivity structure in the deep zone. Therefore, discontinuity F1 seems to have developed only in the shallow zone.

The low resistivity zone which shows less than 5ohm-m is not recognized in the area to the west of discontinuity F2.

#### c. Resistivity Discontinuity F3

Resistivity discontinuity F3 runs from the area between station 2 and 6 to the area beside station 5 roughly in a E-W direction roughly.

Discontinuity F3 is recognized in the resistivity map of low resistivity layers and the depth map of the resistivity basement, but is not recognized from two-dimensional modeling results (resistivity maps and resistivity sections). Thus, a more detailed survey will be needed to estimate whether a fracture system exists or not along this discontinuity.

#### d. Resistivity Discontinuity F4

Resistivity discontinuity F4 runs from the west of El Cedro to the area beside station 6 roughly in a ENE-WSW direction.

Since resistivity discontinuity F4 is clearly recognized in the resistivity map for a depth of 1500m, that at 3000m deep, which show the resistivity

structure in the deep zone, and the resistivity sections (④ ~ ⑥), the discontinuity F4 probably reflects a fracture system developed in the deep zone. The discontinuity runs almost parallel to discontinuity F1 and the uplifted structure of the resistive zone at depth is clearly recognized between discontinuity F1 and F4. Also the low resistivity zone is distributed on and above this uplifted structure. Therefore, discontinuity F4 probably reflects a fracture system which controls geothermal fluid at depths as is assumed for F1.

e. Resistivity Discontinuity F5

Resistivity discontinuity F5 runs from the area beside station 5 to the area beside station 48 passing through the eastern end of Laguna de Calderas roughly in an ESE-WNW direction.

Since discontinuity F5 is recognized clearly in the resistivity map for a depth of 1500m and that for 3000m, which show the resistivity structure in the deep zone, and resistivity sections (⑨ ~ ⑩), this resistivity discontinuity (F5) is supposed to reflect a fracture system developed in the deep zone. However, low resistivity zones are not distributed and geothermal manifestations are not recognized around the discontinuity F5 in the east of the survey area. Therefore, there seems not to be any active geothermal activity around discontinuity F5 in the east of the survey area.

## 5. Consideration of Magnetotelluric Survey Results

a. Resistivity Structure at Shallow Depths in the Survey Area

Fig.2-2-12 shows the resistivity discontinuities (F1~F5) together with low resistivity zones showing less than 6 ohm-m obtained from the resistivity map of low resistivity layers. The low resistivity zones in this map show a relatively shallow resistivity structure roughly in the range from 200m to 700m deep.

In this map, a low resistivity zone showing less than 6 ohm-m is distributed roughly along and between resistivity discontinuity F1 and F4 excluding the area around Laguna de Calderas. Since some thermal manifestations such as fumaroles and altered zones are recognized at the ground surface in the low resistivity zone including the locations of the AMF-2 well and El Cedro, this low resistivity zone is considered to reflect a hydrothermally altered zone in the relatively shallow zone. Specifically, it is considered that the geothermal fluid coming from a deep area along fracture zones around or beneath the low resistivity zone formed the hydrothermally altered zone in the relatively shallow zone. The area around Laguna de Calderas seems to be affected by cold water coming into the caldera structure, and thus the area is a high resistivity zone.

Since no low resistivity zones are distributed in the east of the survey area, there seem not to be any geothermal systems which contain large amounts of high temperature fluid in the east of the survey area.

b. Resistivity Structure at Deep Depths in the Survey Area

Fig.2-2-13 shows the resistivity discontinuities (F1~F5) together with

high resistivity zones showing more than 20 ohm-m obtained from the resistivity map for a depth of 1500m. Considering the resistivity distributions in each resistivity section, the resistive zones in this map seems to reflect an uplifted structure of the resistive zone at depth.

In this map, a resistive zone is clearly distributed in the central portion, northeast portion and east portion of the survey area. And the uplifted structure of the resistive zone at depth seems to be distributed and surrounded by discontinuities F1, F4 and F5. In particular, a high resistivity zone is clearly recognized in the area between the southwest portion of discontinuity F1 (to the south of Laguna de Calderas) and discontinuity F4. Therefore, an uplifted structure of the resistive zone at depth is considered to exist between F1 and F4.

Moreover, the resistivity structure in the shallow zone described before indicates a remarkable low resistivity zone, which probably reflects a hydrothermally altered zone and which is distributed on and above the uplifted structure between F1 and F4. Furthermore, the wells AMF-1 and AMF-2 which were successfully drilled to produce geothermal fluid are located between the discontinuities F1 and F4. Therefore, it is highly probable that fracture systems are well developed along and between the discontinuities F1 and F4 and the geothermal fluid in the deep zone flows up along these fracture systems.

c. Summary of the survey results

Five resistivity discontinuities (F1 ~ F5) were obtained from the magnetotelluric survey results. In particular, a remarkable low resistivity zone which may reflect a hydrothermally altered zone is distributed along and between discontinuities F1 and F4. And the wells (AMF-1, AMF-2) which were successfully drilled to produce geothermal fluid are located between discontinuities F1 and F4. Therefore, fracture systems in the deep zone are probably developed along and between discontinuities F1 and F4 at depth.

Based on these results, we estimate that the geothermal fluid at depth flows up along the fracture systems which are located along and between discontinuities F1 and F4, and some of the geothermal fluid trapped in the relatively shallow zone is likely to form a hydrothermally altered zone along and between discontinuities F1 and F4.

In conclusion, the area along the southwest portion of discontinuity F1 (to the southwest of the Laguna de Calderas) and the area along discontinuity F4 can be recommended as promising zones for future drilling targets.

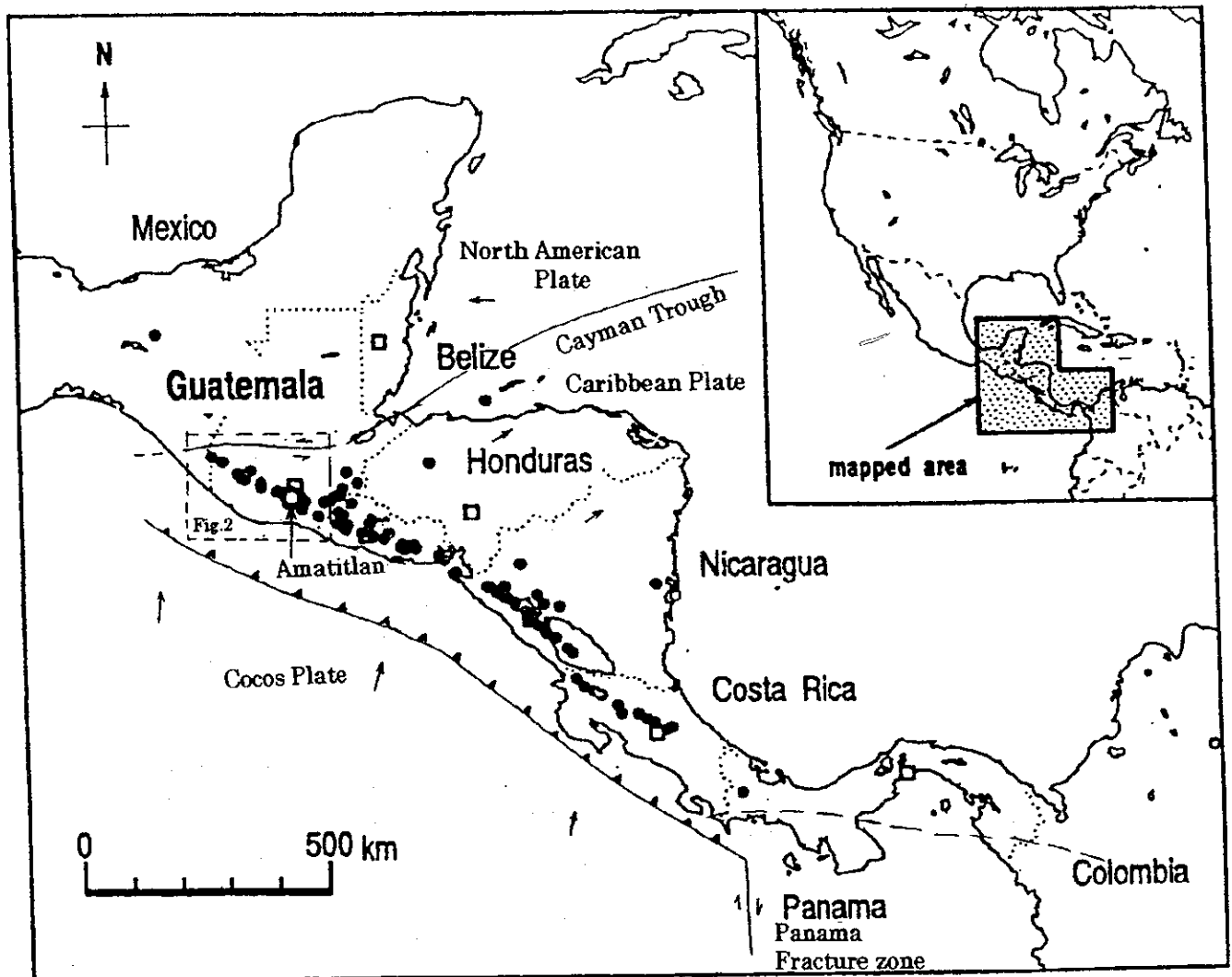


Fig. 2-2-1 中央アメリカの火山列

Volcanic chain in Central America

Solid circle shows volcano active in Holocene (Simkin et al, 1981), and open square show capital. Pacaya Volcano, show in open circle, is located in the north of the volcanic chain. (Modified with S. Kitamura and O. Matis, 1995 and Molnar and Lynn R, 1969)

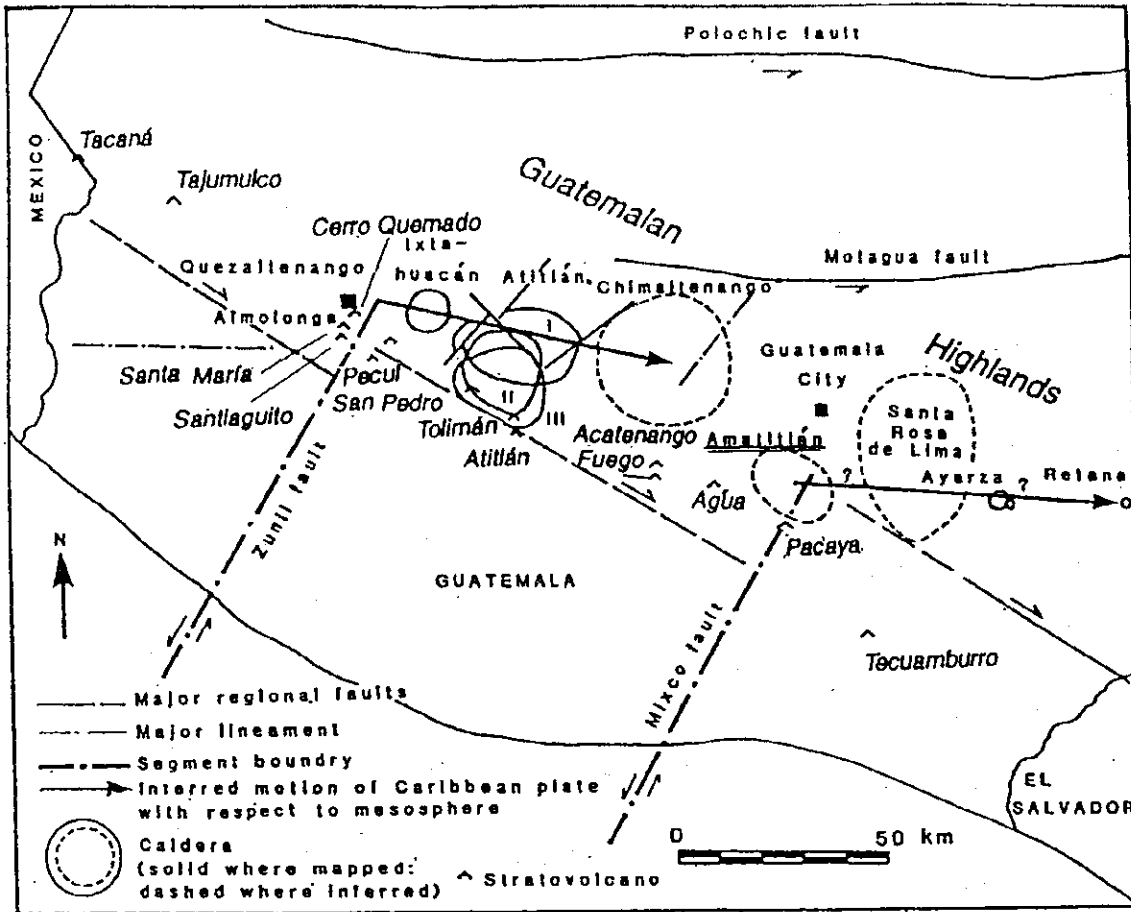


Fig. 2-2-2 広域地質構造図

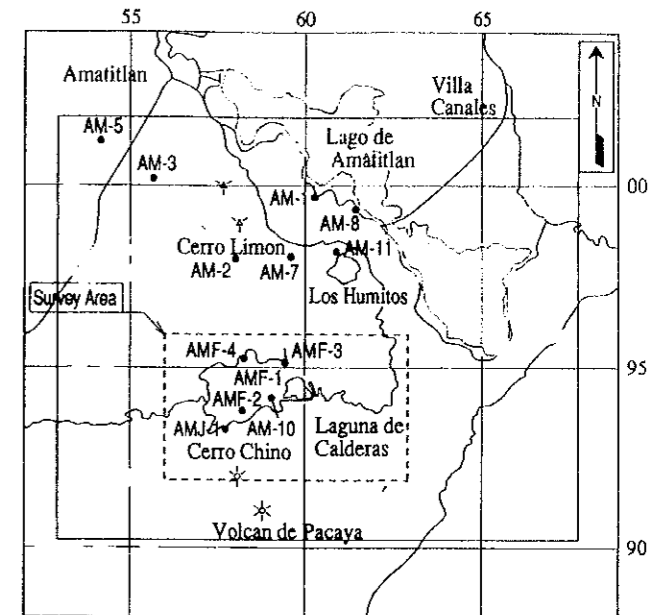
### Regional tectonic map

Apparent migration of loci of caldera formation toward the WNW and SSW. Apparent WNW trend is interpreted as a track of calderas formed above present location of V. Almolonga, astride the Zunil fault. Apparent SSW trend is interpreted as generation of successive calderas at intersection of a proto-Zunil fault (now beneath the Atitran complex) and the volcanic front, as the volcanic front "migrated" trenchward. All migration is interpreted as a consequence of ESE movement of the Caribbean plate relative to the subduction zone and mesosphere at a rate of 0.4cm/yr.

(Modified with C.G Newhall, 1987 and Vallance et al, 1995)







Legend abbrev.	Stratigraphy	Formation and Rock Type	Description	Age
AC		Alluvium and Colluvium	Sand, gravel and Volcanic fall deposit, mainly black volcanic Lapilli	
Pv	Pacaya Volcanic Complex	Younger Pacaya Volcanics	Dark Black, porous, scoriaceous basaltic Lapilli and lava	
Op		Older Pacaya Volcanics	Dark gray, porous, scoriaceous basic Andesite lava	4-8Ka
Pd		Dome and Acidic lava flow	Milk-white-pale brown, porous, Pliofite and Calcite, with gray, acidic andesite	61±0.9Ka 9.98-0.11Ma
Sf		San Vicente Pacaya Fall deposits	Alternations of milk-white-pale brown, porous pumice fall deposits and dark black-dark gray, in-h-hardness, scoriaceous fall deposits	40-90Ka 0.15Ma
Et	Post-Caldera formation	Basaltic scoria and lava	Dark black-dark gray, basaltic scoria and lava	
Lp	Amatitlan Volcanic Complex	Los Humitos Volcanic Pyroclastics	Milk-white-pale brown, pyroclastics, strong altered Andesite rock perfolites and rhyolitic pumice	
Ap		Amatitlan Volcanic Pyroclastics	Milk-white-pale brown, pyroclastics with, rarely Andesite blocks, mainly rhyolitic pumice	55Ma
Hv		Hoja de Ocoso Volcanics	Red-red purple, andesite lava, Pz rich with small dark minerals	
Av		(Post-Caldera Formation) Ancient Volcanics	Dark gray-gray, partially altered Px andesite lava	1.06Ma
Cp	Syn-Caldera formation	(Syn-Caldera Formation) Volcanic Pyroclastics	Brown-yellow brown, pyroclastics partially with weathered andesite block, Lacustrine sediments (clay-silt sand rarely basaltic scoriaceous fall deposits)	
Cf		(Syn-Caldera Formation) Andesite Lava flow	Dark gray, weakly altered Andesite, with medium-coarse grained Pz	
Ag	Pre-Caldera formation	Pre-Agua Volcanics	Dark gray, Pz Andesite lava and Andesite Pyroclastics, partially covered with silica deposits near hot-spring	
Gr		Basement Rocks	Pale brown, weakly altered and weathered Granite with, coarse grained Pz and Qtz (partially Fragmentic)	14.1±0.8Ma 15.2±0.8Ma

Pz : Plagioclase Qtz : Quartz Px : Pyroxene

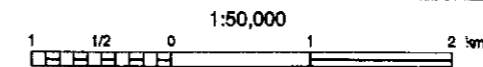
	Alteration zones, Fumarole zones		Crater
	Hot springs, Fumaroles		Phreatic Centre
	(Estimated) Fault		Lineament
	Morphological escarpment (Aerophoto Analysis) Downthrown side		Survey area
	Cross section		

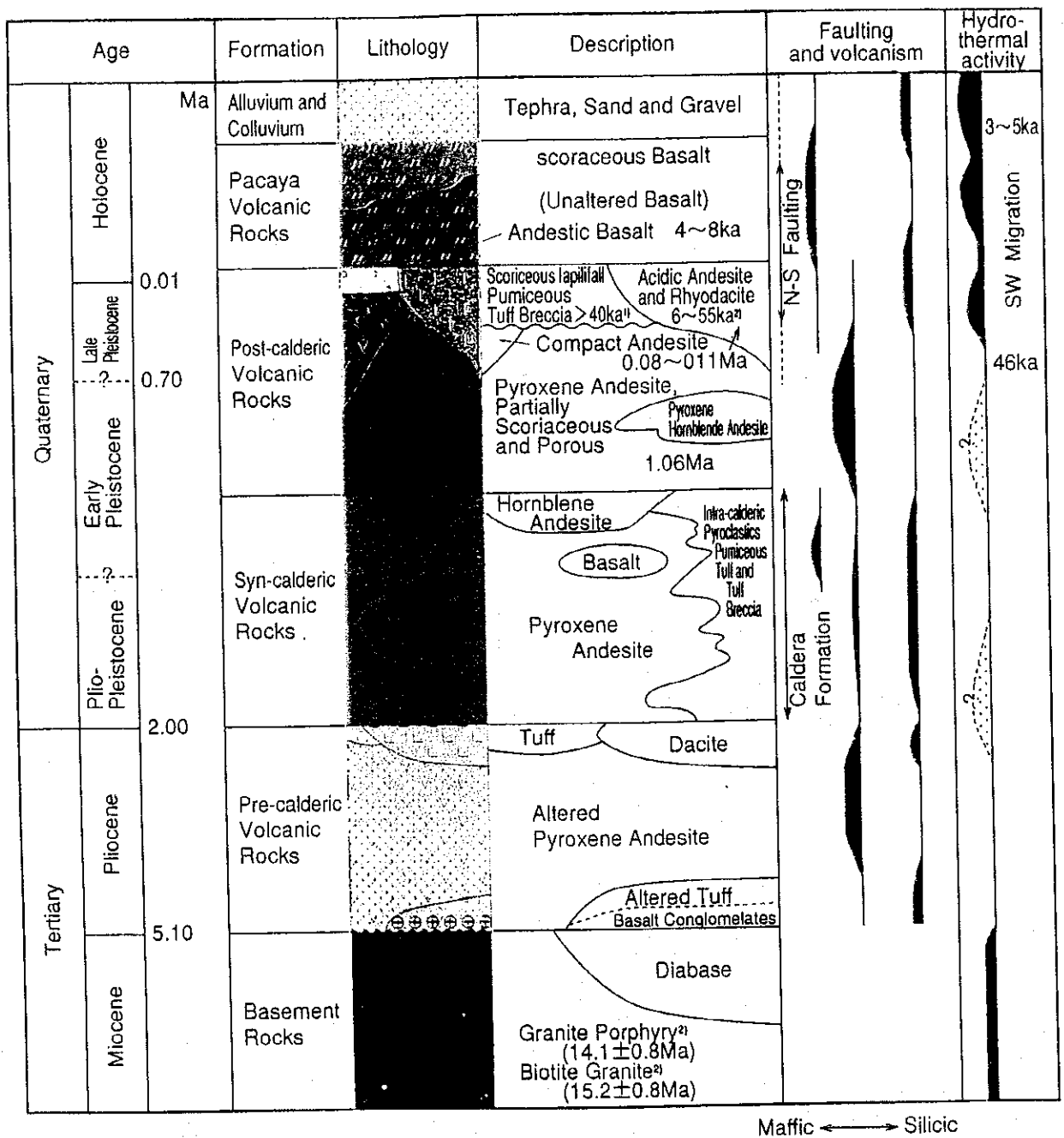
**Amatitlan Geothermal Field**

地 質 図

**Geological Map**

JICA-WEST JEC Fig. 2-2-3





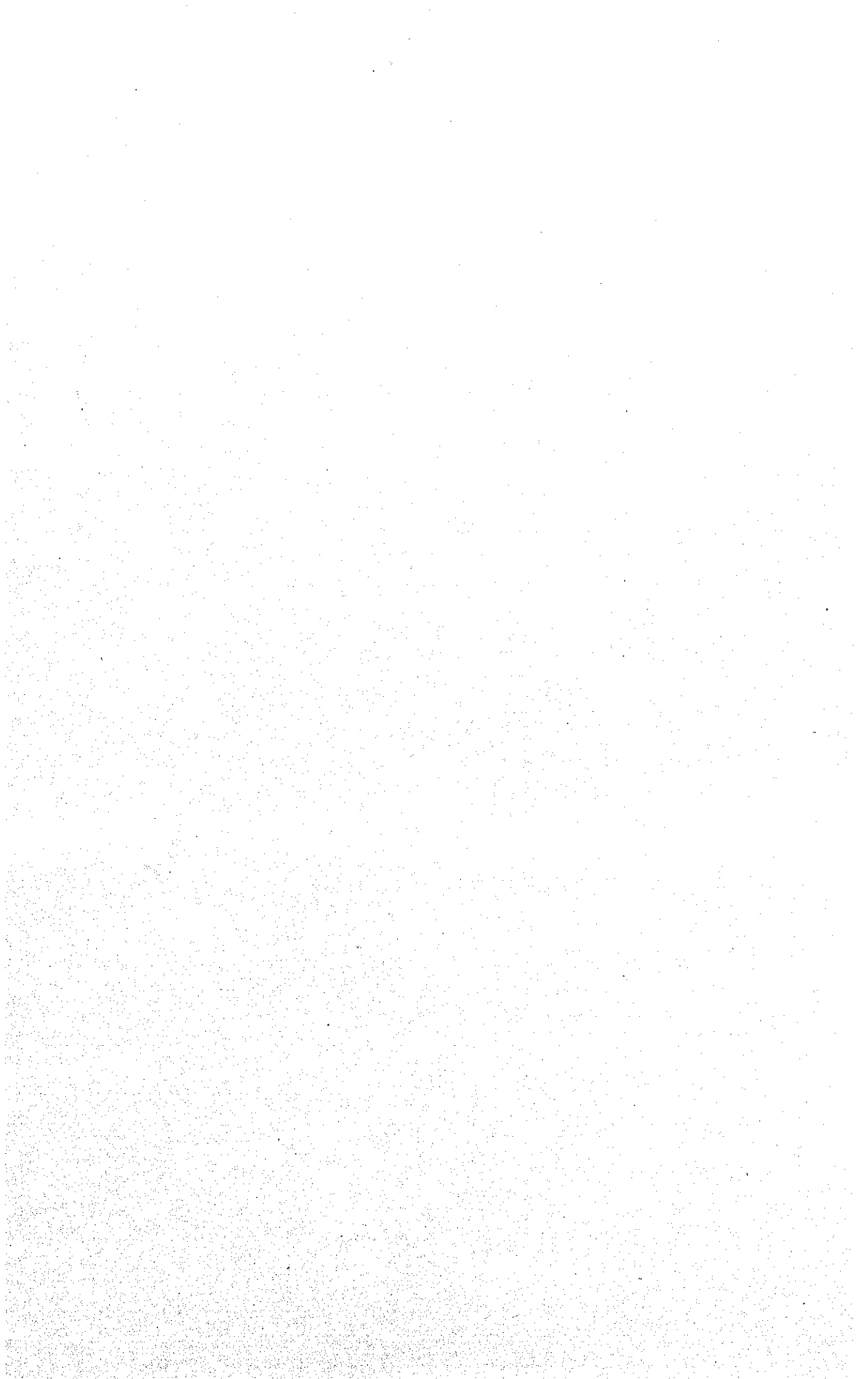
Reference

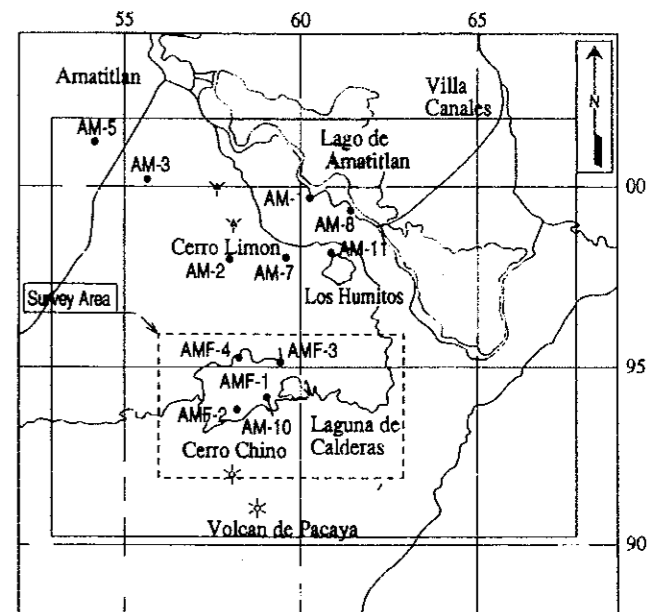
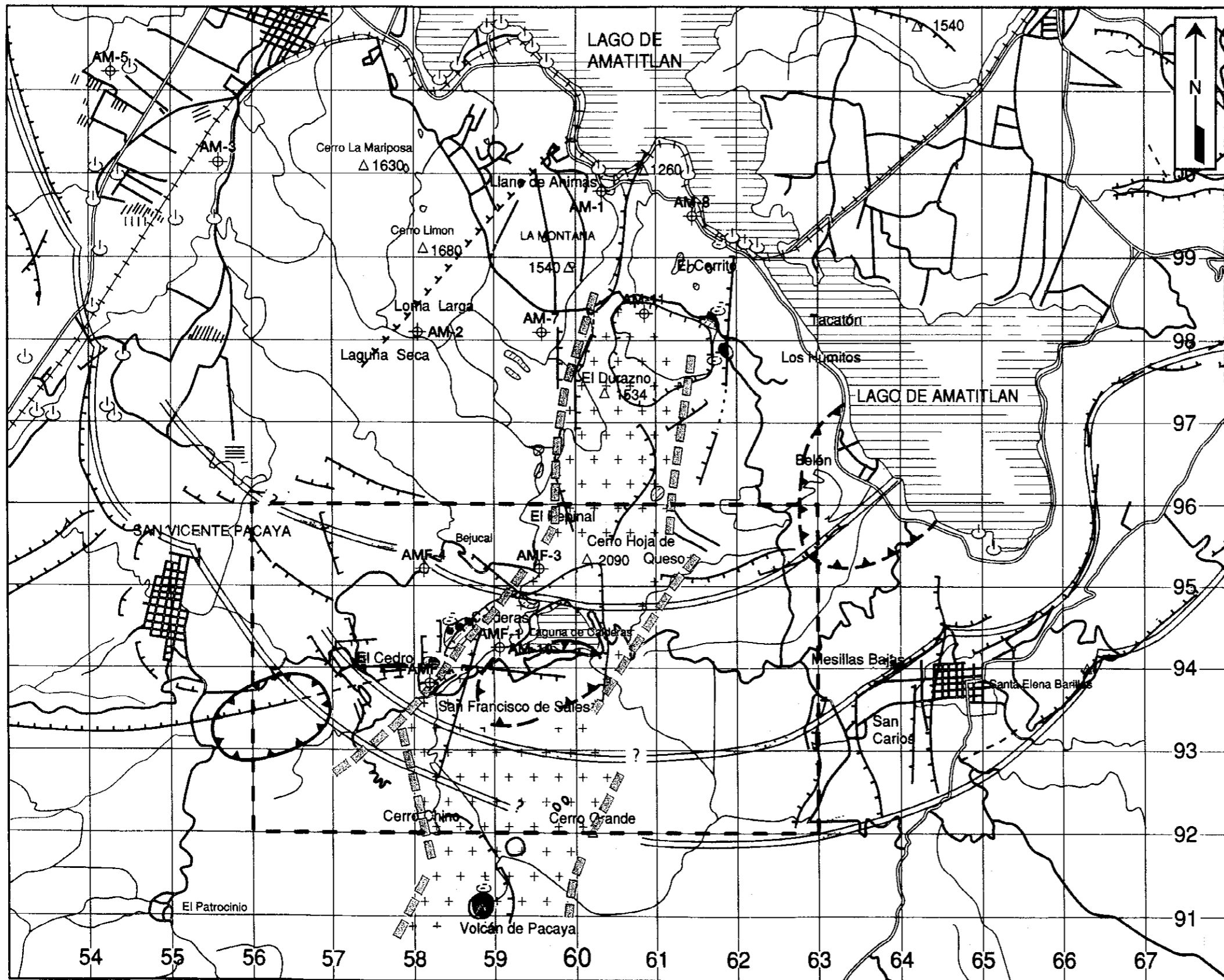
1) Koch and Mclean, 1975

2) West JEC and Telectro, 1994 and this report

Fig. 2-2-4 アマティラン地熱地域の地質層序

Stratigraphy of the Amatitlan geothermal field





- Legend**
- Estimated uplift obtained from gravity survey
  - Estimated basin obtained from gravity survey
  - Caldera Wall

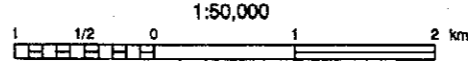
	Alteration zones, Fumarole zones		Crater
	Hot springs, Fumaroles		Phreatic Centre
	(Estimated) Fault		Lineament
	Cross section		Survey area

Amatitlan Geothermal Development Project

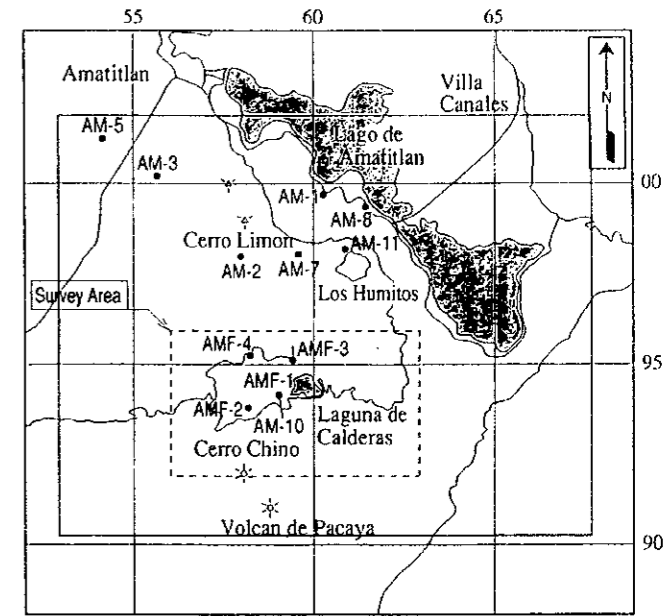
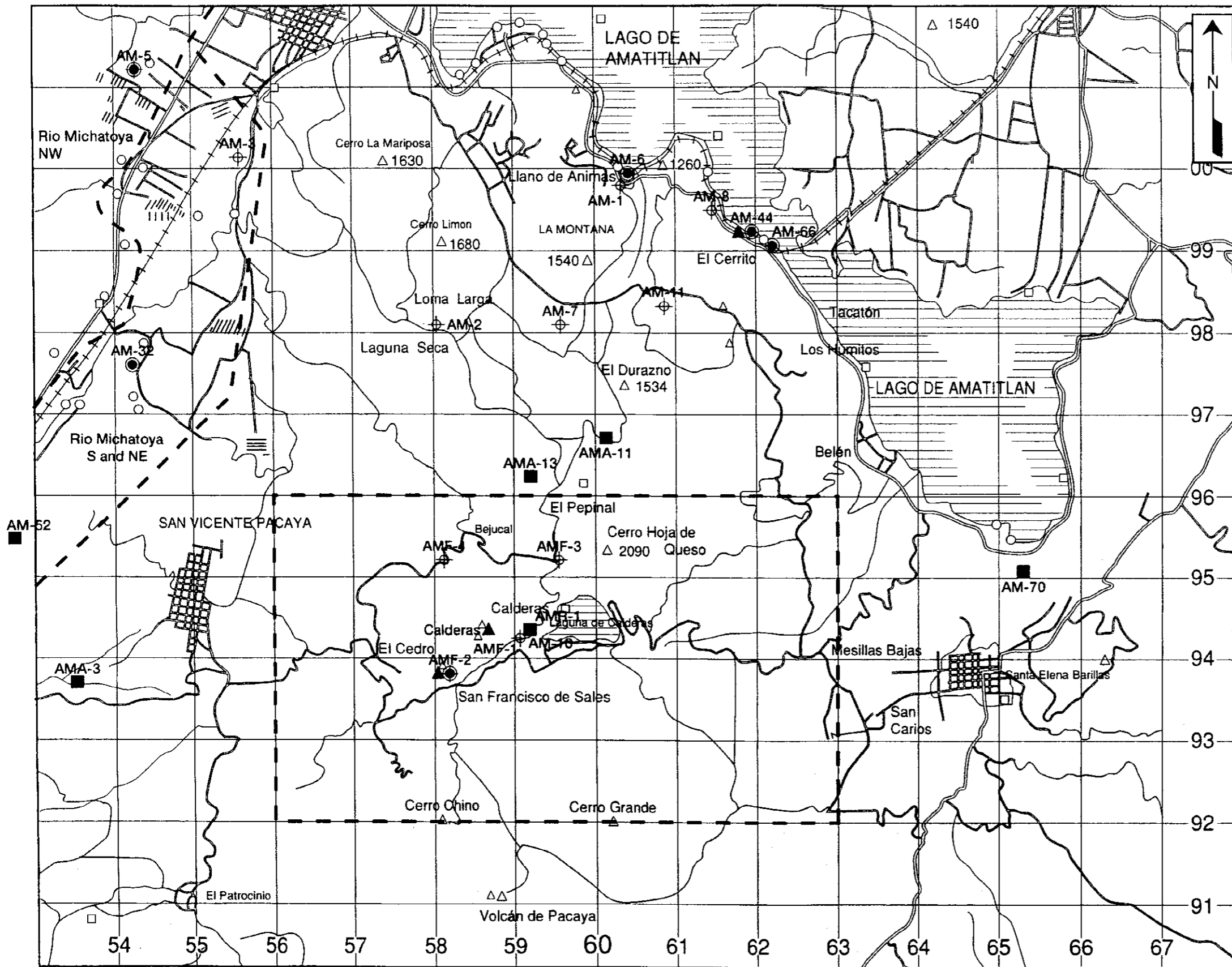
地質構造図

Geological Structure

JICA-WEST JEC      Fig. 2-2-5

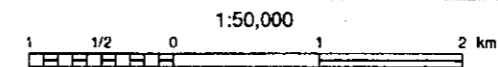


M88101-001A



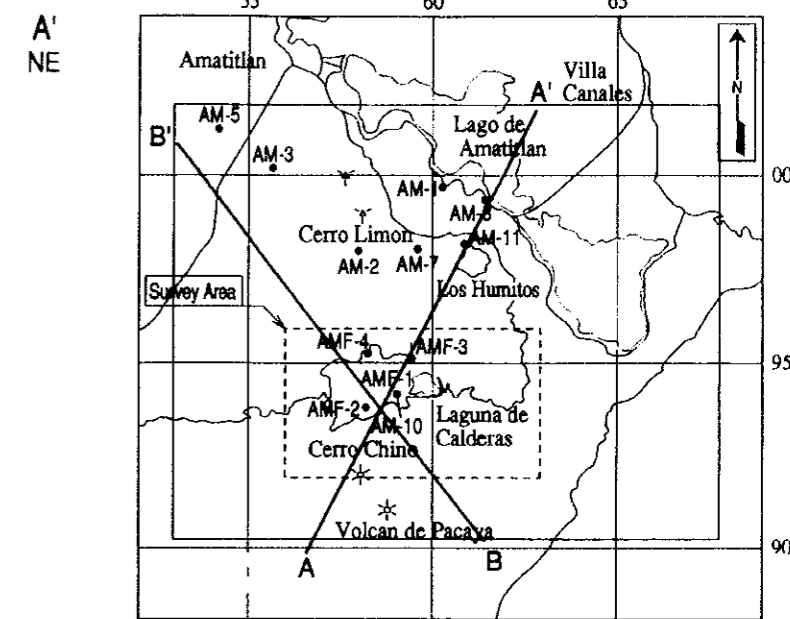
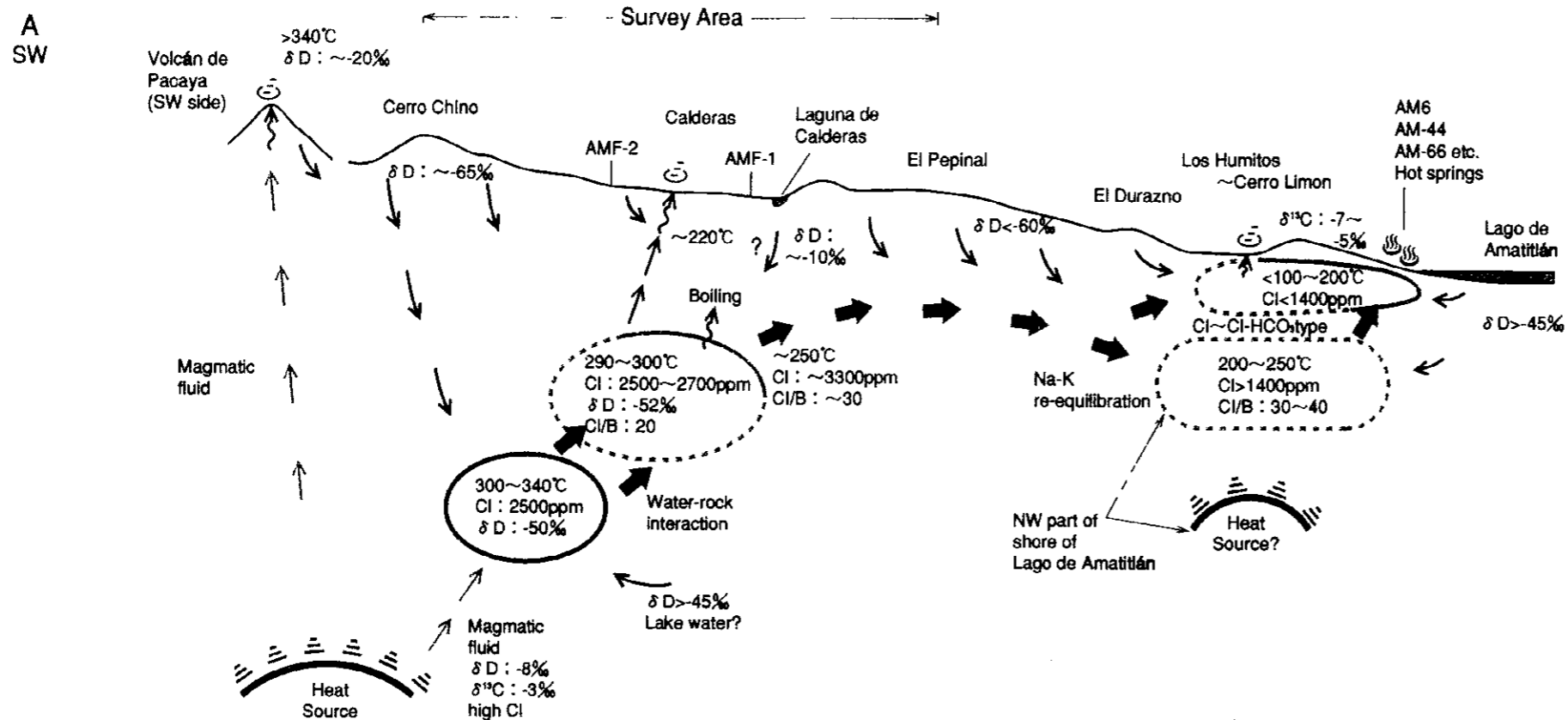
**LEGEND**

- Hot Spring Water, Well Hot Water (6points)
- Surface Cold Water (6points)
- ▲ Fumarolic and Bubble Gas (3points)
- Survey Area
- ⊕ Existing Well
- Existing Data
- Hot Spring water, Well Hot Water
- Surface Cold Water
- △ Fumarolic Gas



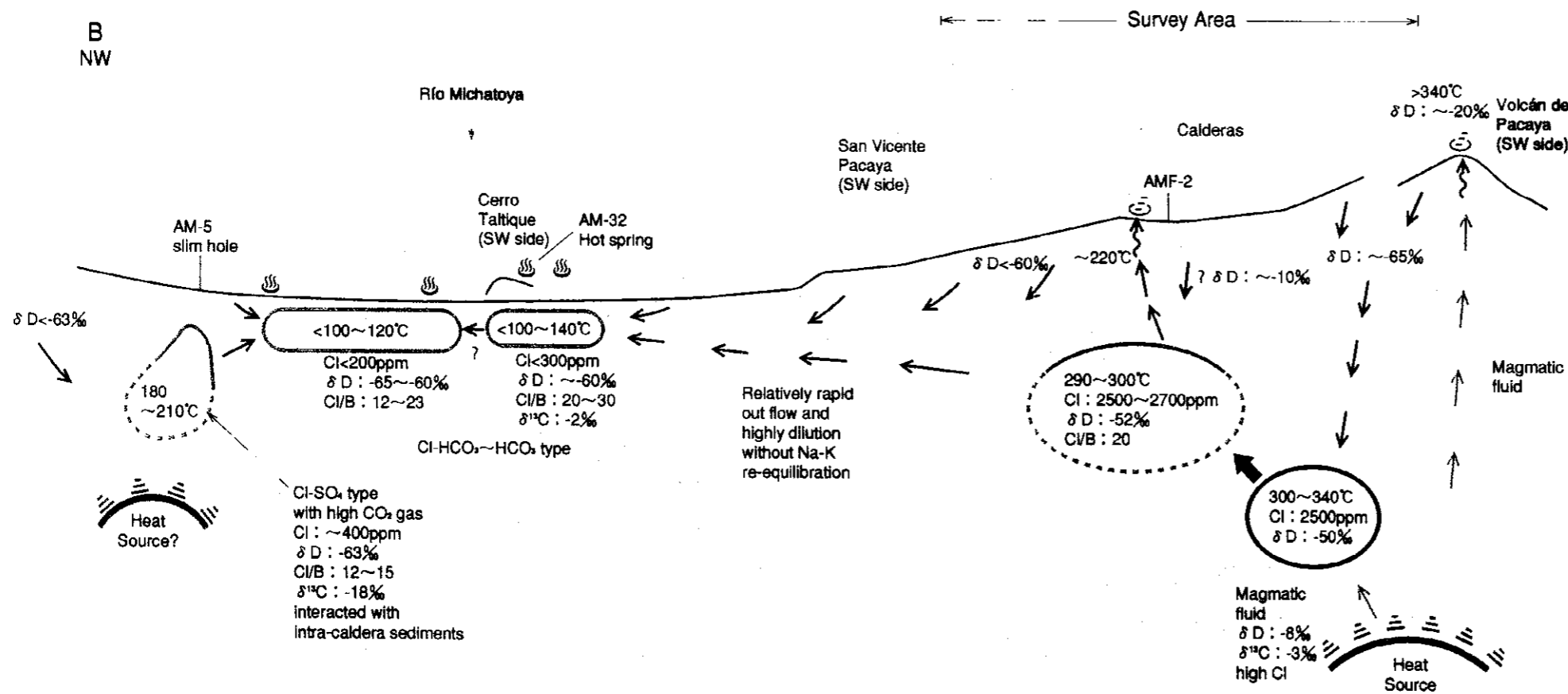
Amatitlan geothermal development project	
分析用流体試料採取位置図	
Location map of fluid samples for analysis	
JICA-WEST JEC	Fig. 2-2-6

M98101401A



**LEGEND**

- High temperature reservoir
- Low temperature reservoir (Hot spring aquifer)
- Parental fluid of the Amatitlán geothermal system
- Thermal water flow
- Boiling and steam flow
- Meteoric cold water flow

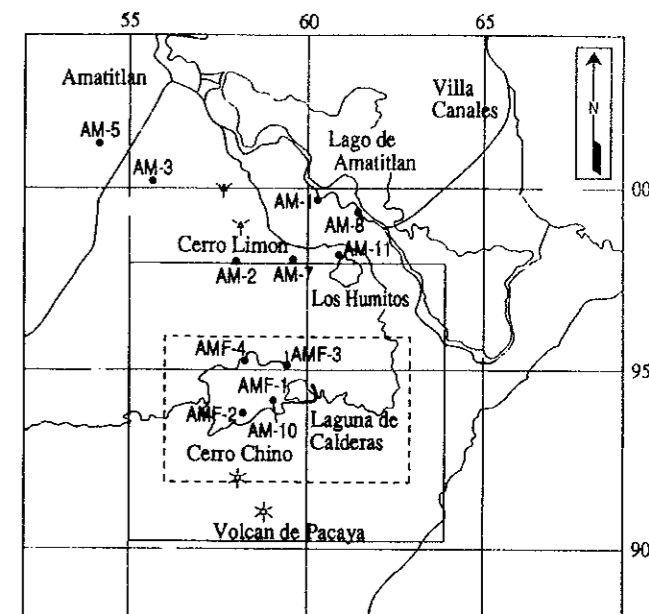
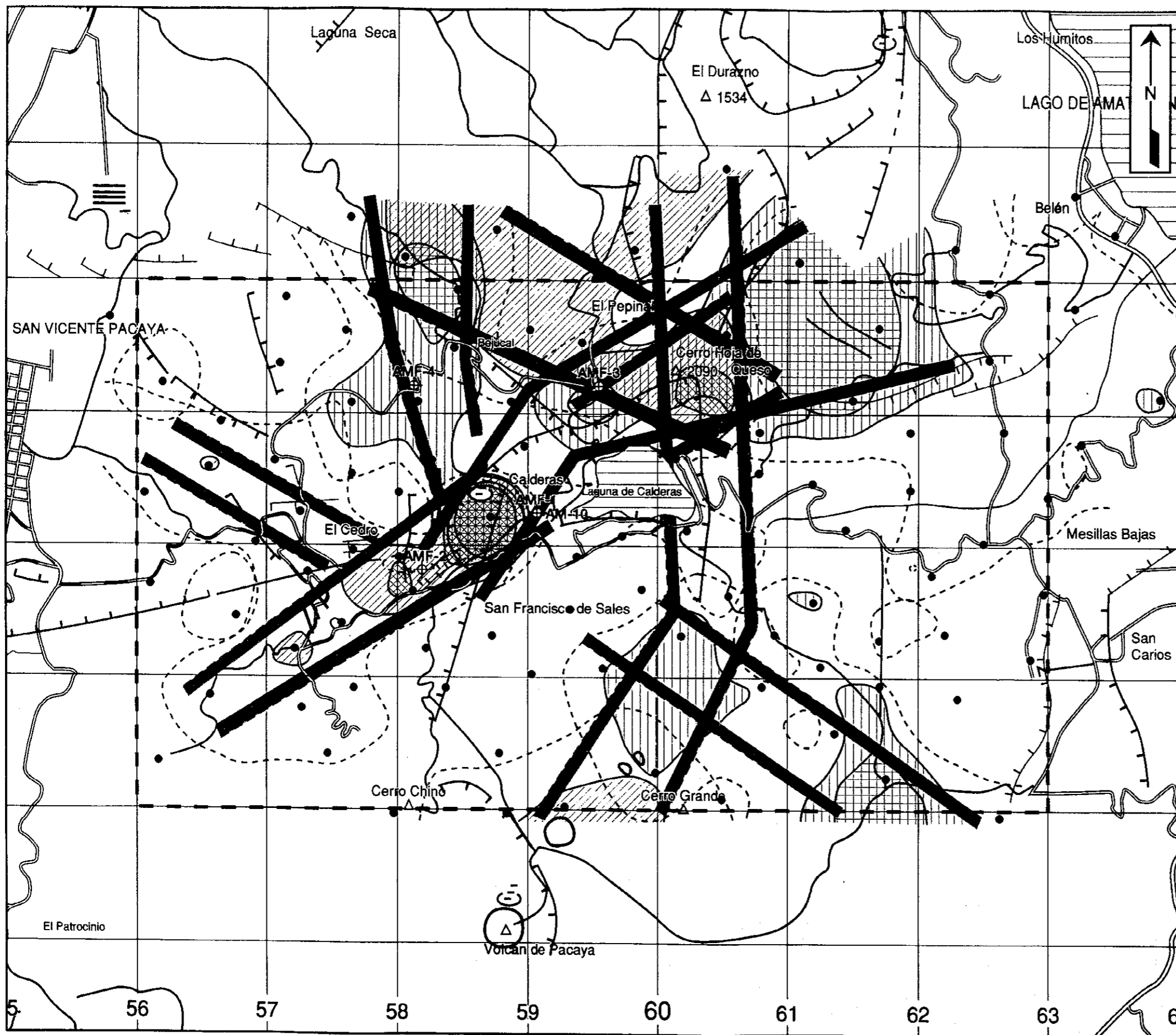


Amatitlán geothermal development project






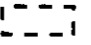



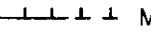
熱水系地化学モデル図

Geochemical model of hydrothermal system

JICA-WEST JEC Fig. 2-2-7



LEGEND

-  Permeable Zone Based on Hg Distribution
-  Hg Anomaly
-  Permeable Zone Based on Corrected Distribution
-  Corrected Rn Anomaly
-  Sampling Station (109 points)
-  Survey Area
-  Existing Well
-  Fault, Caldera Wall
-  Crater
-  Morphologic Escarpment

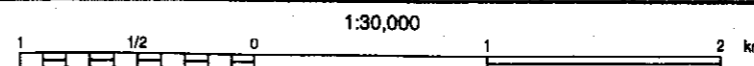
Amatitlan geothermal development project

土壤ガス調査による高透水性ゾーン集約図

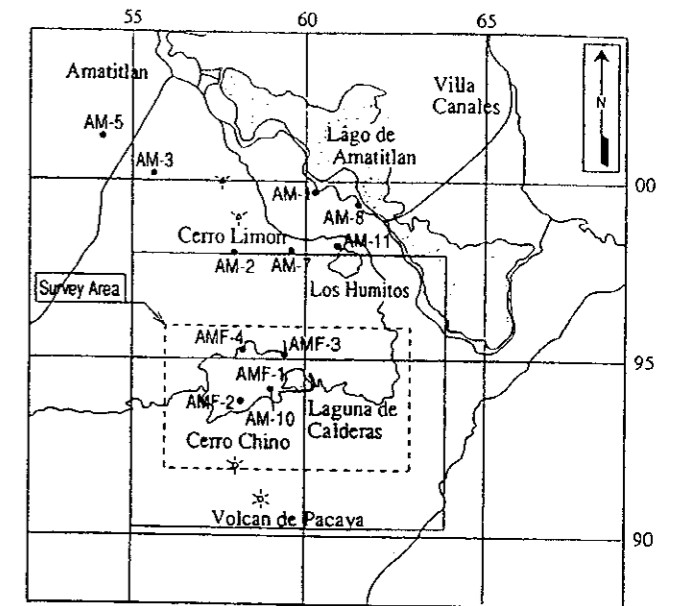
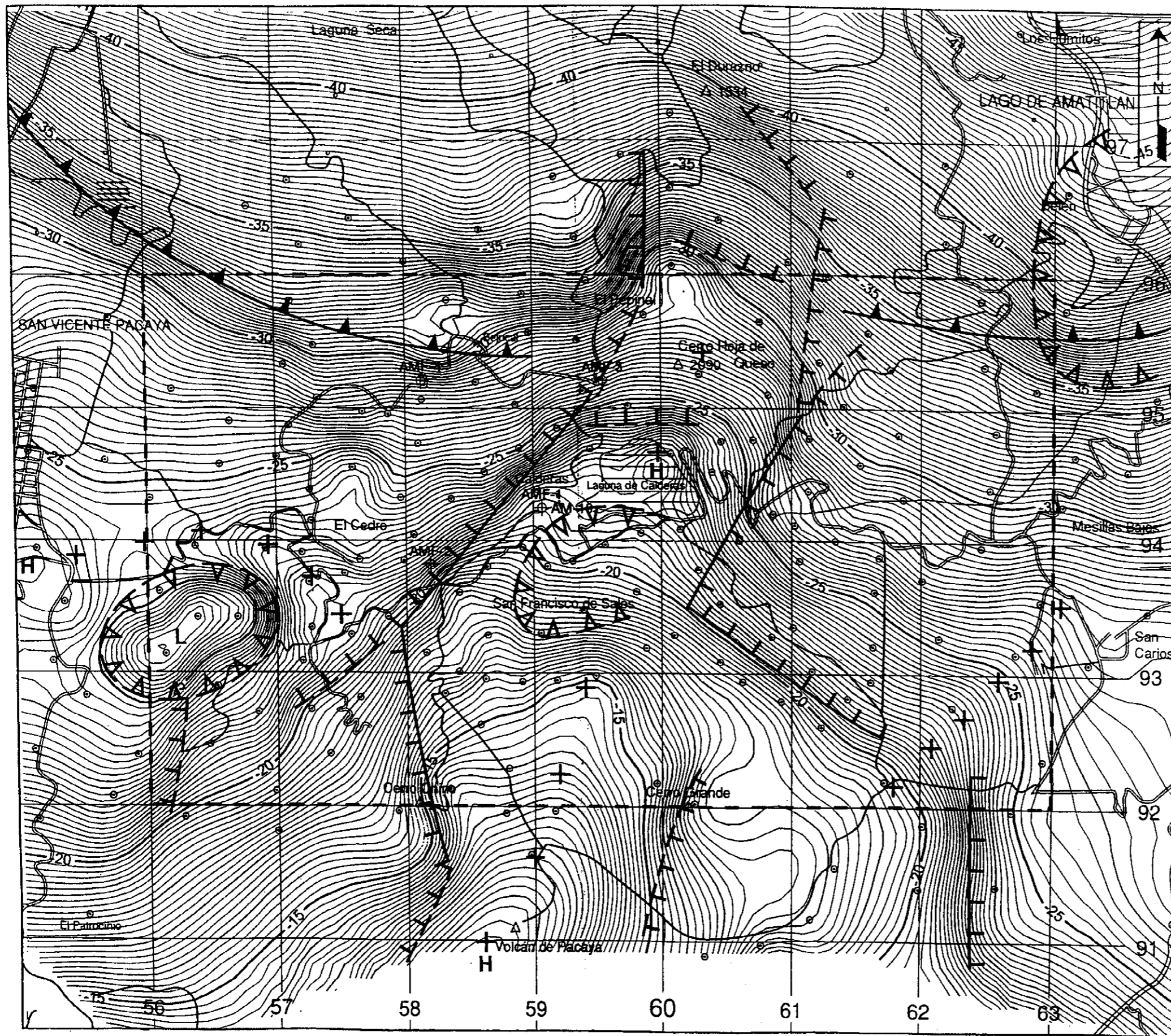
Compiled map of permeable zone by soil-gas survey

JICA-WEST JEC

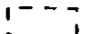






Fig. 2-2-8



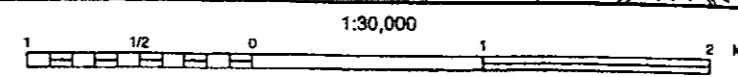


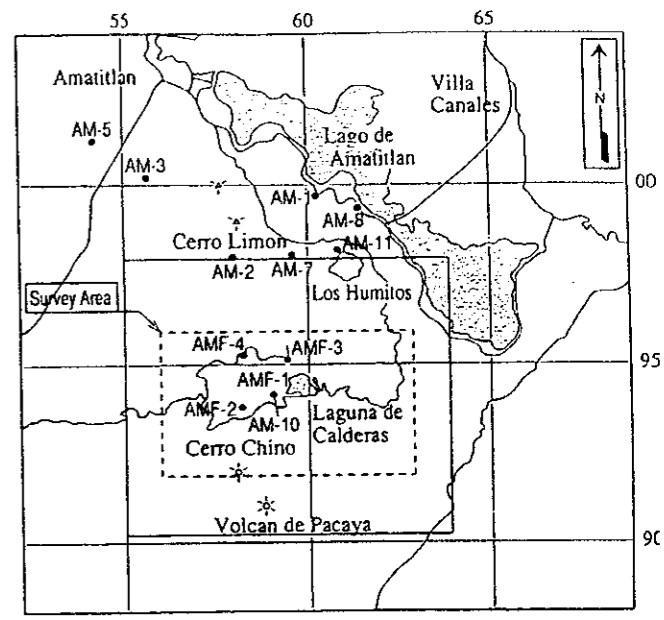
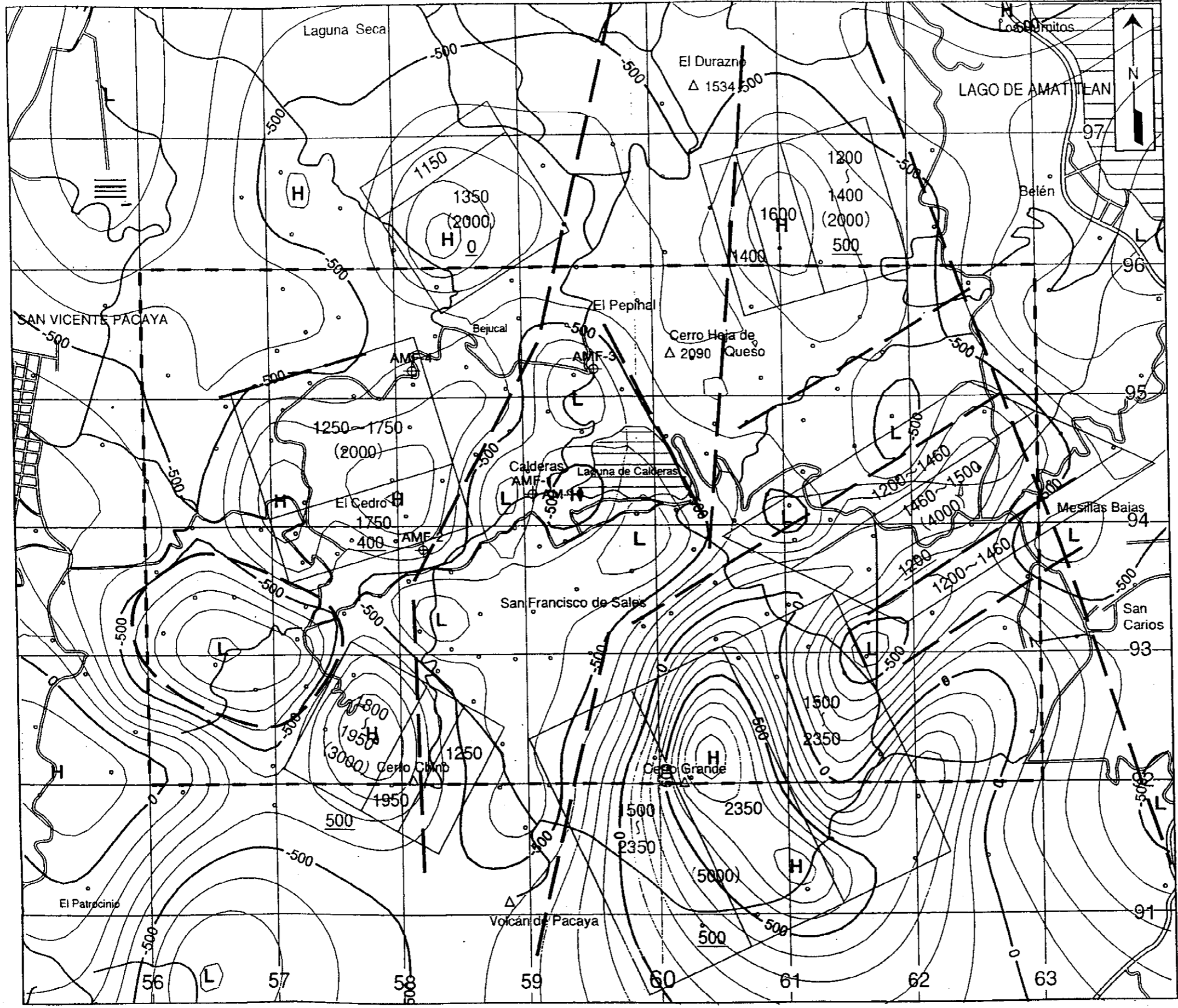


Legend

-  : Survey Area
-  : Exploratory Well
-  : Caldera Rim Estimated from Gravity
-  : Basin
-  : Gravity Lineament(major)
-  : Gravity Lineament(minor)
-  : Basement Uplift trend

Amatitlan Geothermal Development Project	
重力解析図	
Gravity Interpretation Map	
JICA-WEST JEC	Fig. 2-2-9

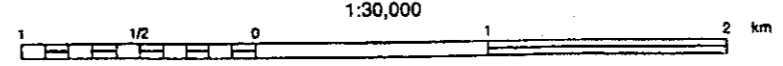


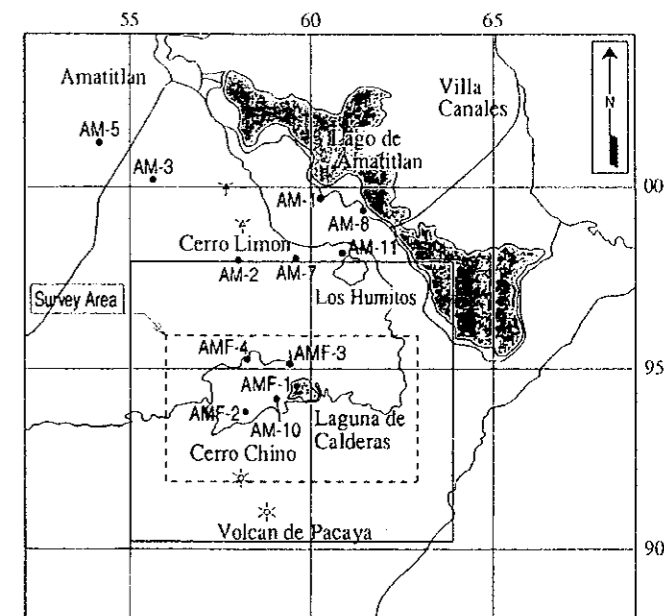
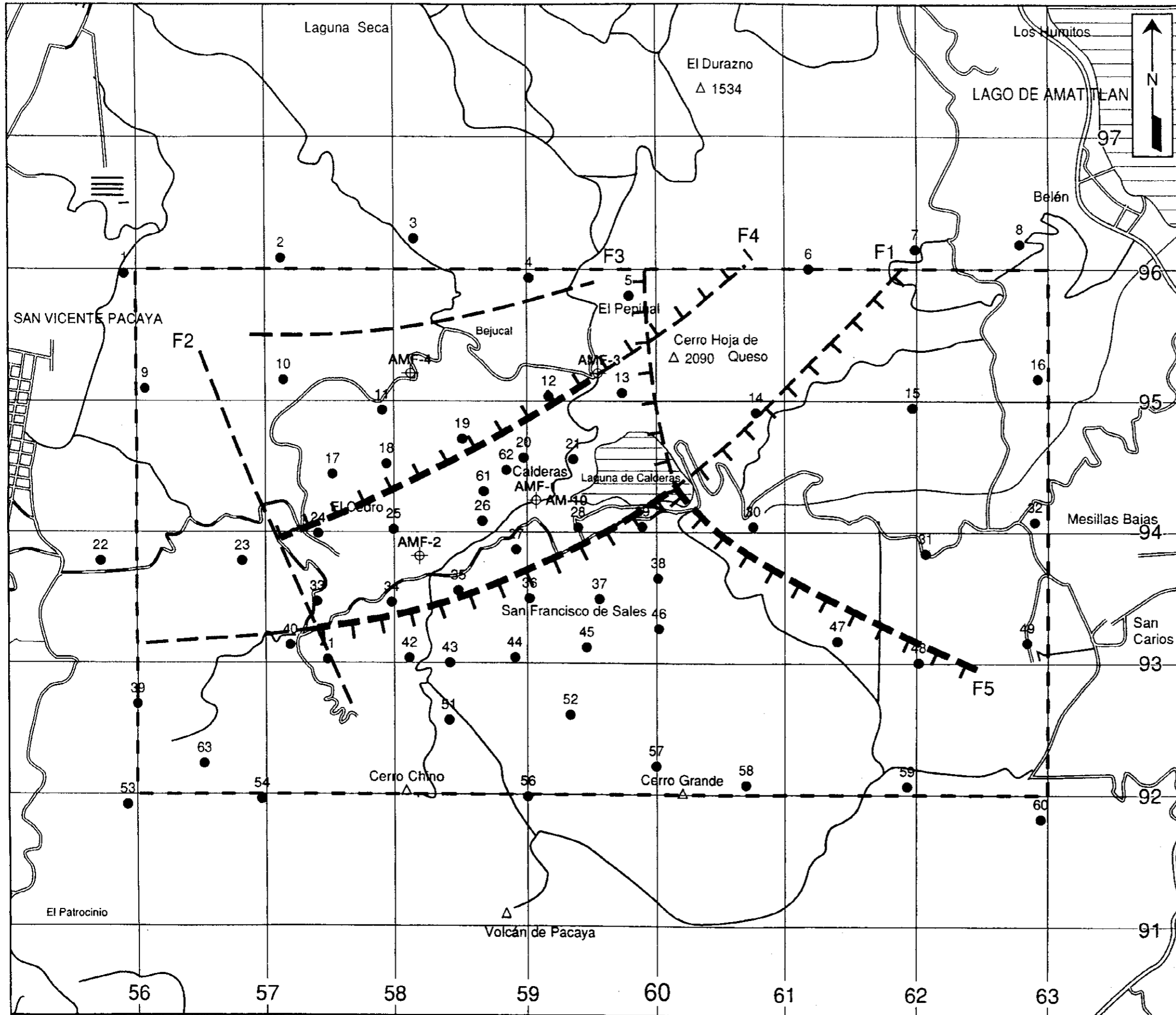


Legend

- - - : Survey Area
- ⊕ : Exploratory Well
- - - : Magnetic Discontinuity
- : Magnetic Body
- 1600 : Top Depth of Magnetic Body
- (2000) : Magnetic Susceptibility  $\times 10^{-6} \text{emu/cm}^3$
- 500 : Bottom Depth of Magnetic Body

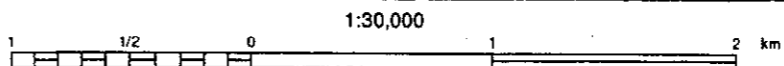
Amatiñan Geothermal Development Project	
磁気解析図	
Magnetic Interpretation Map	
JICA-WEST JEC	Fig. 2-2-10



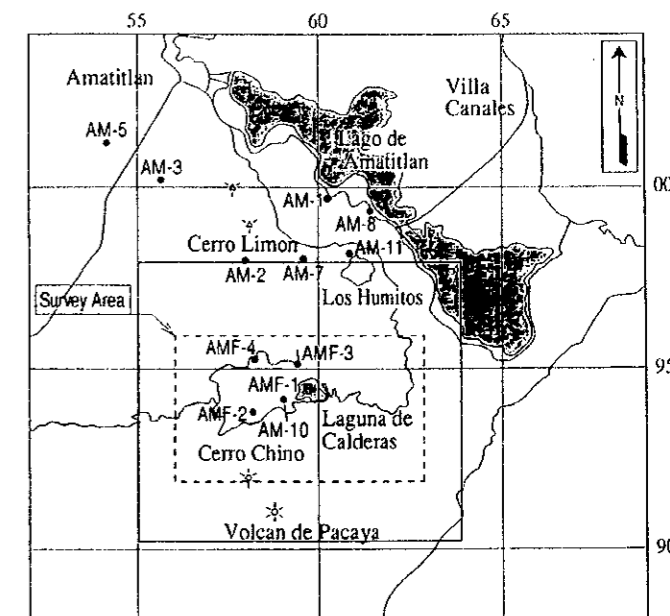
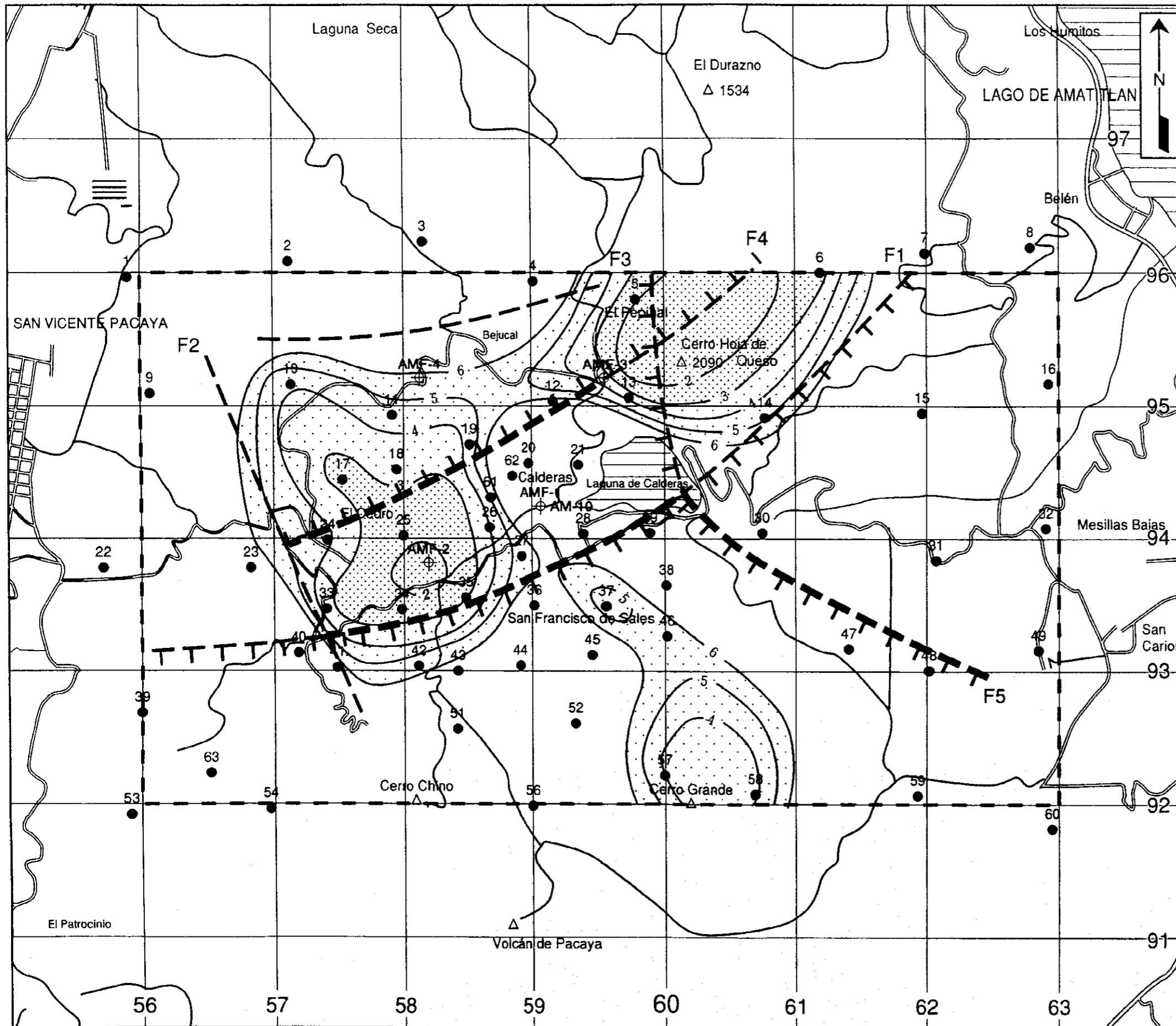


- Legend**
- : Survey area
  - ⊕ : Exploratory well
  - : MT station
  - : Resistivity discontinuity

Amatlan Geothermal Development Project	
比抵抗不連続線分布図	
Resistivity discontinuities distribution map	
JICA-WEST JEC	Fig. 2-2-11



M88101401A



Legend

- : Survey area
- : Exploratory well
- : MT station
- : Resistivity discontinuity
- : Contour line of resistivity (Low resistivity layer, ohm-m)

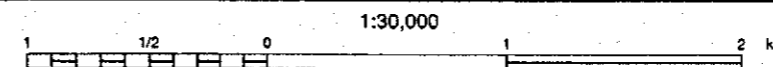
Amatitlan Geothermal Development Project

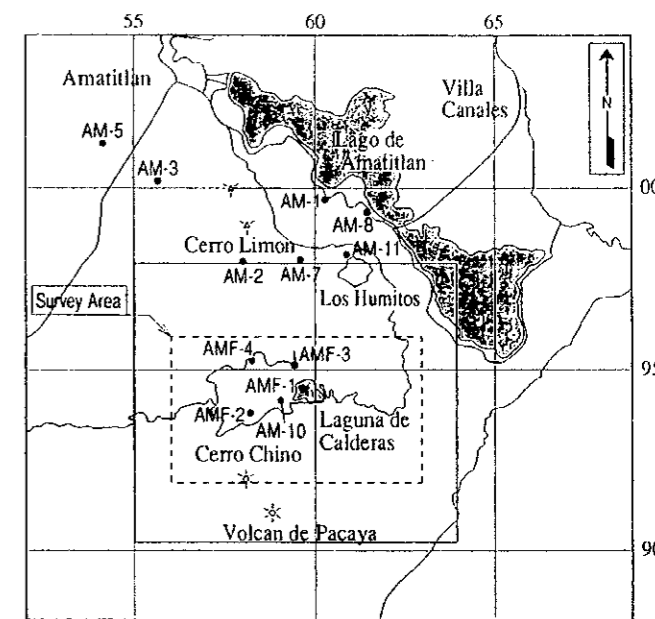
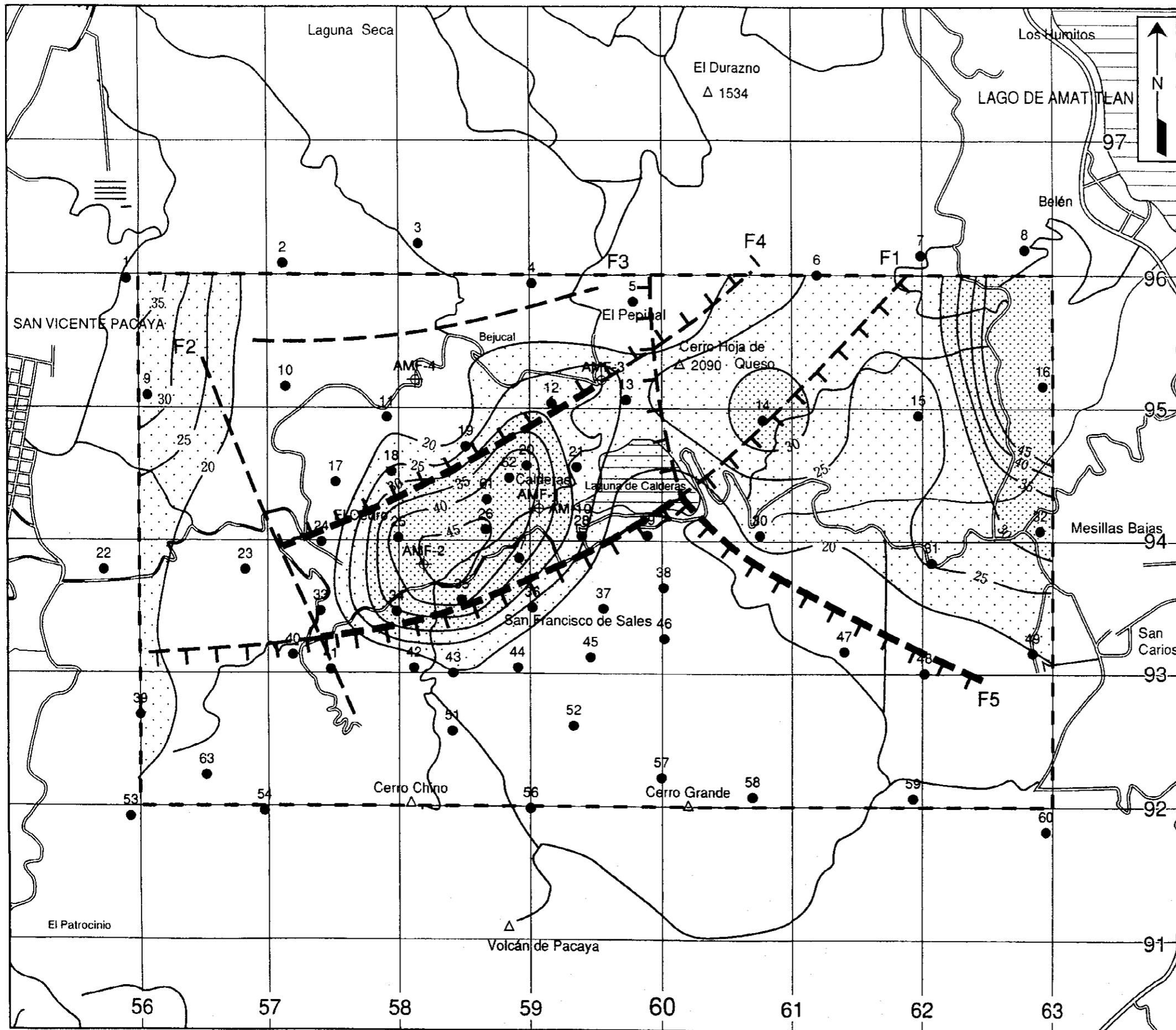
浅部比抵抗構造解析図

Resistivity structure in shallow zone

JICA-WEST JEC

Fig. 2-2-12

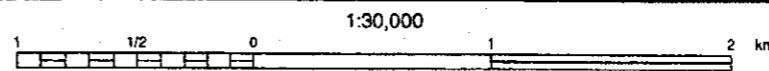




Legend

- : Survey area
- : Exploratory well
- : MT station
- : Resistivity discontinuity
- : Contour line of resistivity (Resistivity distribution at 1500m deep)

Amatitlan Geothermal Development Project	
深部比抵抗構造解析図	
Resistivity structure in deep zone	
JICA-WEST JEC	Fig. 2-2-13



## 2.3 Exploratory Well Drilling

2.3.1 Well AMJ-1

2.3.2 Well AMJ-2

## 2.3 EXPLORATORY WELL DRILLING

### 2.3.1 WELL AMJ-1

#### 1. WORK ACTIVITIES

Based on the "Drilling tender document for an exploratory well in Amatitlan" which was prepared in fiscal year 1998, the international pre-bid meeting and contract negotiation was held in Guatemala City on August, 1999 for the drilling contract for the exploratory well AMJ-1. After the bidding process, Simmons Drilling International, who has much geothermal drilling experiences in Berlin geothermal field in El Salvador, was selected as a winner of the bid.

The drilling operation was started on 23<sup>rd</sup> of December 1999 and terminated on 5<sup>th</sup> February 2000 as a total depth was 1700.5m. The well testing was carried out after running 7-5/8" liner, and the rig was released on 10<sup>th</sup> of February 2000.

The well location is summarized as follows.

	Coordinates	Altitude	Total Depth
AMJ-1	X=757,737 Y=1,593,207	1,885.00m	1,700.50m

#### 2. DRILLING

The mobilization of the drilling equipment and rig-up were completed on December 22, 1999. After drilling of rat hole and mouse hole, drilling of the 17-1/2" hole was started at 16:30 on December 25. During the drilling of the 17-1/2" hole, two loss zones at 2m and 8m were encountered and first one was treated with LMC, another was treated with two cement plugs. Drilling was continued with 17-1/2" bit to 10m where the very hard formation was encountered. From 10m, 12-1/4" hole was drilled to 32m with normal condition. After reamed to 32m with 17-1/2" bit, reaming with 26" hole opener started from 2m. During reaming with 26" hole opener at 11.4m, a partial loss of circulation zone was encountered. The formation washout was found at the shoe of 30" conductor pipe, and a cement plug was set to prevent the cave-in hole. After reaming cement to 11.4m, the 20" casing was run to 10.8m and cemented on January 1, 2000. After waiting on cement set for 20 hours, the 30" conductor pipe and 20" conductor casing were cut and a 20" well head, 21-1/4"-2000# BOP, flow line were installed.

A 17-1/2" bit was run in hole after the opening and closing test of annular BOP. The top of cement was tagged at 7m and reaming cement started on January 3. After reaming cement and open hole to 32m with 17-1/2" bit, the drilling of the formation started with same bit. During drilling in this period, two partial loss zones were encountered at 83m and 151m, and they were treated with LCM successfully. Drilling was continued to a depth of 300.2m with 17-1/2" bit without problem. After finished drilling, a wiper trip was made to the 20" casing shoe to check hole condition. On January 9, the 13-3/8" casing was run in to a depth of 295.7m and cemented. During cementing

operation, partial loss of circulation was occurred in the open hole. After waiting on cement set for 24 hours, the top cement job was carried out in the annular space between the 20" casing and 13-3/8" casing because of the falling of the top of cement. After three top cement job, the 13-3/8" casing was cut and a 13 3/8"-2000# casing head was welded to the 13-3/8" casing. A 13 5/8"-5000# annular BOP and a double ram BOP were installed on the casing head.

The pressure test of the wellhead system including BOP was carried out at 600 psig. for 15 minutes. A 12-1/4" bit was run in and tagged the top of cement at 275m on January 12. The drilling of the formation was started after reaming cement to 300.2m and continued to 807.2m without problem. After drilling to 807.2m, the first temperature and pressure logging were carried out to evaluate this interval. The 9-5/8" casing was run in to a depth of 803.3m and cemented on January 20. After waiting on cement set for 24 hours, the 9-5/8" casing was cut below the 13-3/8" casing head and a 10"-600# master valve and BOP were installed on the casing head.

The pressure test of the wellhead system was carried out at 600 psig for 15 minutes. A 8-1/2" bit was run in and tagged the top of cement at 777m on January 23. The drilling of the formation started after reaming cement to 807.2m and the first loss zone was encountered at 1011m. The loss rate was 3m<sup>3</sup>/hr. and drilling was continued with low viscosity mud. Several loss zones were encountered at 1,168m, 1,231m, however those were partial loss zones. Finally, a total loss zone was encountered at 1,493m. Drilling was continued with total loss, however the loss rate was gradually decreased to 20m<sup>3</sup>/hr. or less. After drilling to 1,700.5m with partial loss, the second logging was carried out to evaluate the well and a total depth was declared based on the results of the meeting with INDE and JICA team. After drilling to a total depth of 1,700.5m, 7- 5/8" liner, including 294.26 meters of slotted liner and 637.25 meters of blind liner, was run in and hanged from 756.9m to 1,690.0m. After setting 7-5/8" liner, three hydro-fracturing test were carried out so as to improve permeability of open hole, and a better result was obtained. The water loss test and pressure transient test was carried out with a Kuster tool on February 10. On same day, the 10" master valve was closed, finally rig was released.

### 3. SUMMARY

The results of the drilling AMJ-1 were summarized as follows.

- 1) Total drilling depth was 1,700.5m as compared the programmed depth of 1,500m.
- 2) High temperature geothermal reservoir was encountered below 1,500m.
- 3) Final recovery temperature of the formation was estimated around 300°C.
- 4) The permeability of the formation was not so high.
- 5) Not so many loss of circulation zones were encountered in the open hole.



## 2.3.2 Well AMJ-2

### 1. Work Activities

Based on the document "Drilling tender document for an exploratory well in Amatitlan" which was prepared during the activities of the fiscal year 1999, the international pre-bid meeting and contract negotiation was held in Guatemala City on June, 2000 for the drilling contract for the exploratory well AMJ-2. After the bidding process, Perforaciones Integrales Termicas, S.A.(PITSA), who has much geothermal drilling experiences in Zunil and Amatitlan geothermal field in Guatemala, was selected as a winner of the bid.

The drilling operation was started on 26<sup>th</sup> of August 2000 and completed on 4<sup>th</sup> of November 2000. The well testing was carried out after running 7" liner, and the rig was released on 13<sup>th</sup> of February 2000.

The exploratory well, AMJ-2 was drilled at the northern slope of Mt. Cerro Chino as shown in Fig. 3-5. Well AMJ-2 was directionally drilled down to 1,705m, just beside well AMJ-1, 450m apart in WSW direction from AMF-2.

	Coordinates	Altitude	Total Depth
AMJ-2	X=757,732 Y=1,593,213	1,885.00m	1,705.00m

### 2. DRILLING

The mobilization of the drilling equipment and rig-up were completed on August 25, 2000. After drilling of a rat and a mouse hole, drilling of the 17-1/2" hole was started at 24:00 on August 26. During the drilling of the 17-1/2" hole, no loss zone was encountered. Drilling was continued with a 17-1/2" bit to 8m where a very hard formation was encountered. After reaming to 8m with a 26" bit, the 20" casing was run to 8m and cemented on August 27. After waiting on cement set for 24 hours, the 30" conductor pipe and 20" conductor casing were cut and a 20" well head, 21-1/4"-2000# BOP, flow line were installed.

A 12-1/4" bit was run in hole on August 29. The top of cement was tagged at 7m and continued to ream cement to 8m and drill formation to 13m with same bit. After 13m, pulled out the 12-1/4" bit to the surface to change bit to a 17-1/2". Two partial loss zones were encountered, one at 105m and the other at 156m. First one was plugged with drilled cuttings. While treating the second loss zone, the drill pipe was fallen in the hole with bit and other bottom hole assembly. Immediately the fishing tools such as over-shot, fishing basket were run in hole to recover the fish. However the some trial was resulted unsuccessfully and followed two cement plugs from the bottom to 119m to carry out side-tracking the hole. The side-track was carried out at 119m with a down-hole motor successfully. After side-track, the drilling was continued to a depth of 300m with a 17-1/2" bit without problem. On September 28, the 13-3/8" casing was run in to a depth of 293.4m and cemented. During cementing operation, partial loss of circulation was encountered. After waiting on cement set for 24 hours, the top cement job was carried out in the annular space between the 20" casing and 13-3/8" casing because of the falling of the top of cement. After two top cement job, the 13-

3/8" casing was cut and a 13 3/8"-2000# casing head was welded to the 13-3/8" casing. A 13 5/8"-5000# annular BOP and a double ram BOP were installed on the casing head.

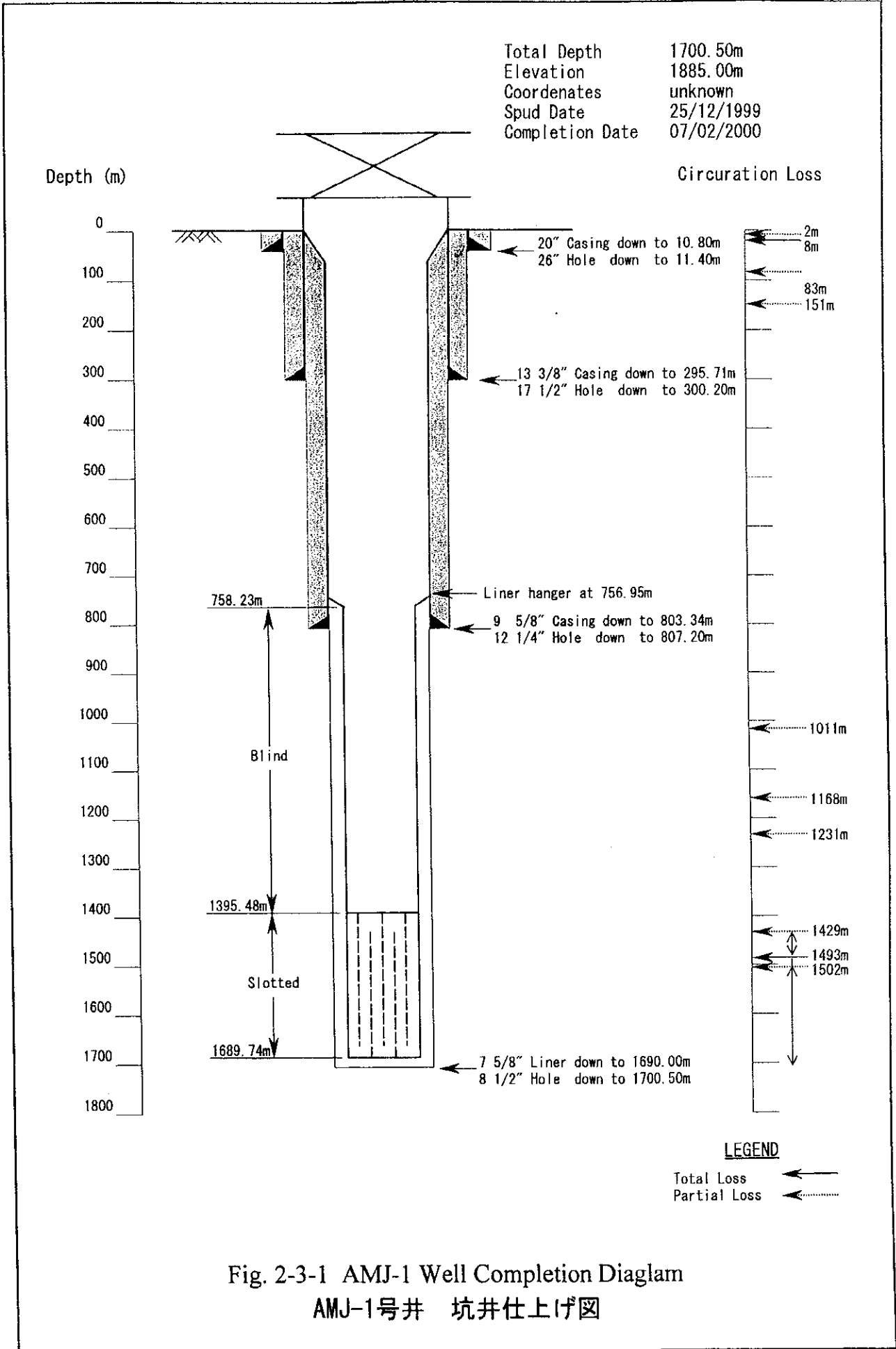
The pressure test of the wellhead system including BOP was carried out at 600 psig. for 15 minutes. A 12-1/4" bit was run in and tagged the top of cement at 271m on October 3. The drilling of the formation was started after reaming cement to 300m and continued to 385m at where the directional drilling was started. The directional drilling was smoothly proceeded to a proposed depth of 1,000m without problem. The 9-5/8" casing was run in to a depth of 996.3m and cemented on October 18. After waiting on cement set for 36 hours, the 9-5/8" casing was cut below the 13-3/8" casing head and a 10"-600# master valve and BOP were installed on the casing head. A top cement job was carried out in the annular space between the 13-3/8" casing and 9-5/8" casing because of the falling of the top of cement.

The pressure test of the wellhead system was carried out at 600 psig for 15 minutes. A 8-1/2" bit was run in and tagged the top of cement at 966m on October 22. After reaming cement to 1,000m, the drilling of the formation was continued to a depth of 1,203m at where the drill strings were stuck. Immediately extra pulling of the strings and oil-spot of the strings were conducted. The oil-spot was so effective to recover the strings successfully. The drilling was continued and the first total loss zone was encountered at 1,539m. At 1,542m, the loss rate was gradually decreased to 20m<sup>3</sup>/hr and the drilling was continued to a total depth of 1705m with partial loss. The 7" liner, including 601.6 meters of slotted liner and 126.6 meters of blind liner, was run in and hanged from 961.1m to 1,690.2m. After setting 7" liner, three hydro-fracturing tests were carried out so as to improve permeability of open hole, and a better result was obtained. The loss rate was improved from 53m<sup>3</sup>/hr to 126m<sup>3</sup>/hr. The water loss test and pressure transient test was carried out with a Kuster tool from November 8 to 13. On November 13, the 10" master valve was closed and the rig was released.

### 3. SUMMARY

The results of the drilling AMJ-2 were summarized as follows.

- 1) Total drilling depth was 1,705m as compared the programmed depth of 1,700m.
- 2) High temperature geothermal reservoir was encountered below 1,539m.
- 3) Final recovery temperature of the formation was estimated around 300°C.
- 4) The permeability of the formation was higher than that of AMJ-2.
- 5) Total drilling days were 80days as compared the programmed days of 70days. The main reason of delay was considered as carried out fishing operations.
- 6) Not so many loss of circulation zones were encountered in the open hole.



Total Depth 1705.00m  
 Elevation 1885.00m  
 Coordinates N: 1,593,213  
 E: 757,732  
 Spud Date 27/08/2000  
 Completion Date 06/11/2000

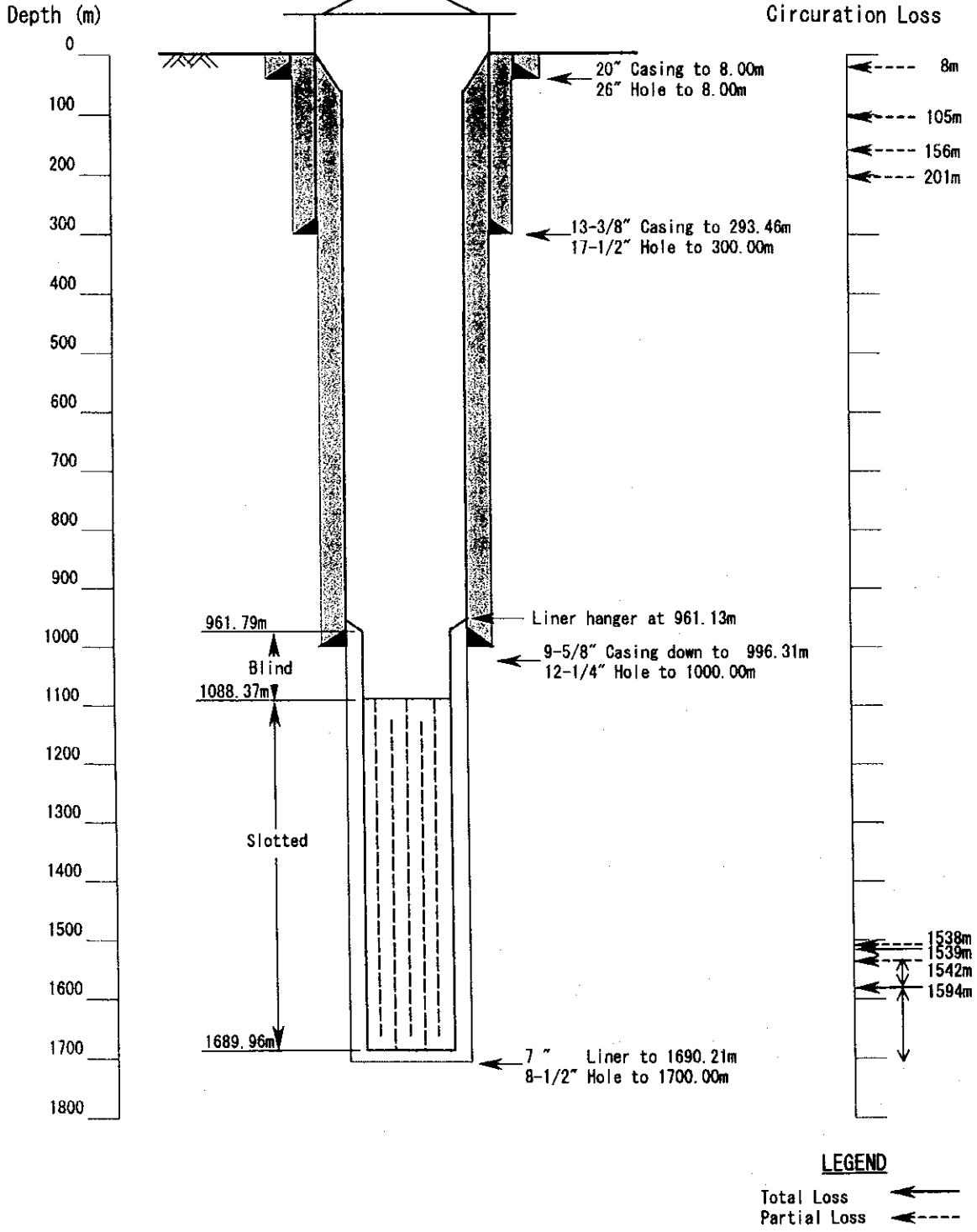
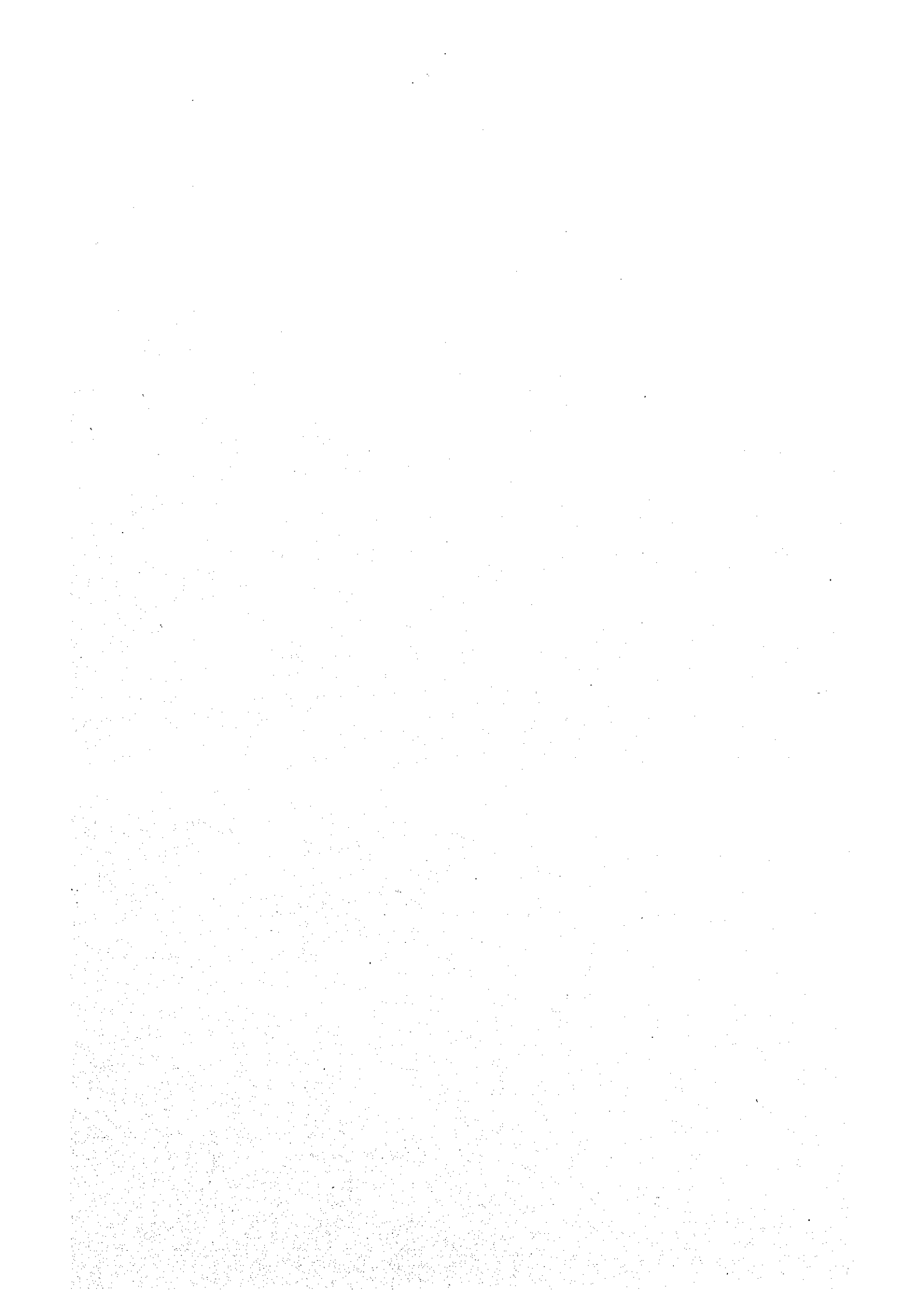


Fig. 2-3-2 AMJ-2 Well Completion Diagram  
 AMJ-2号井 坑井仕上げ図



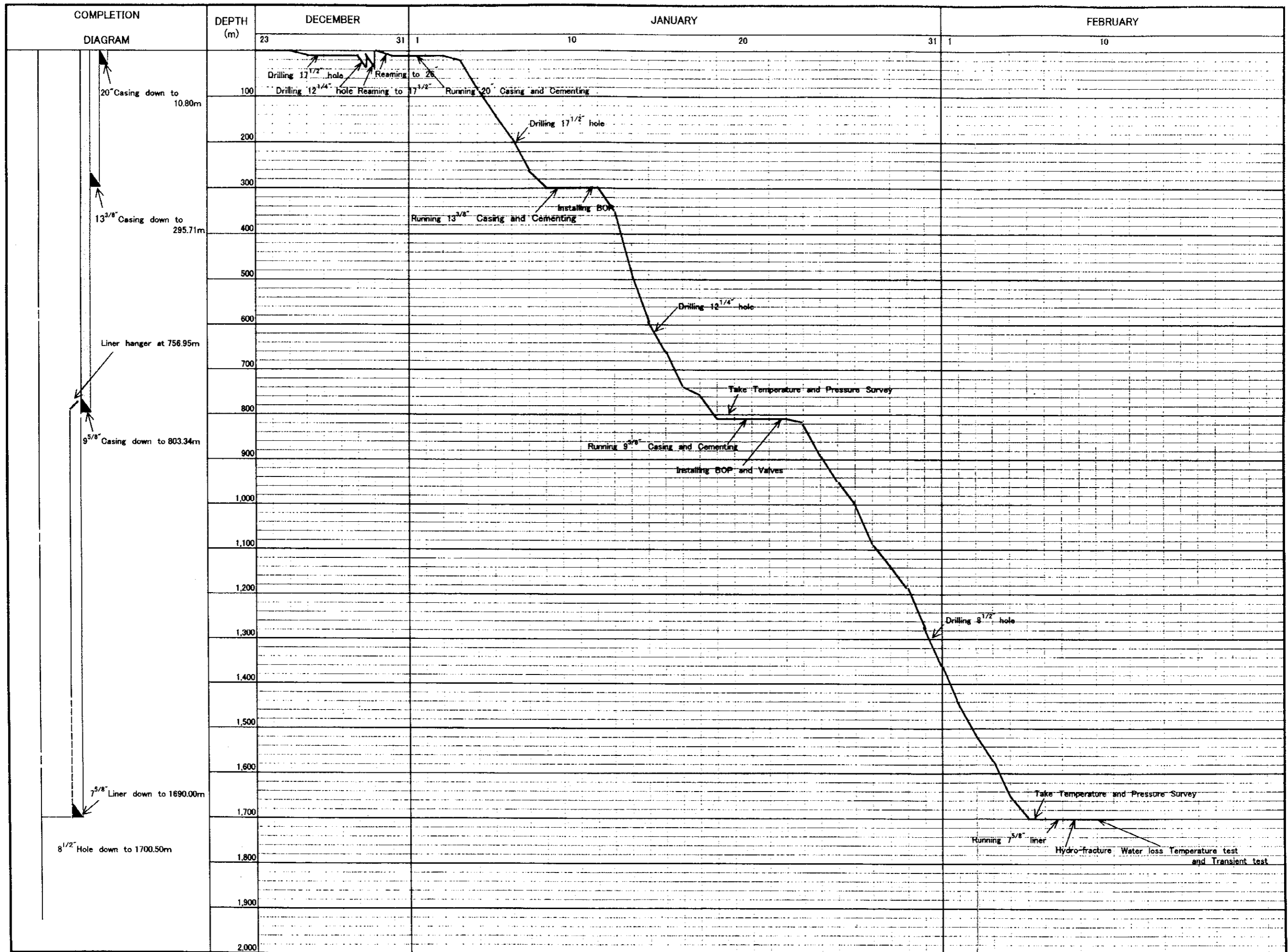


Fig. 2-3-3 AMJ-1 Well Drilling Diagram

AMJ-1号井 掘削実績

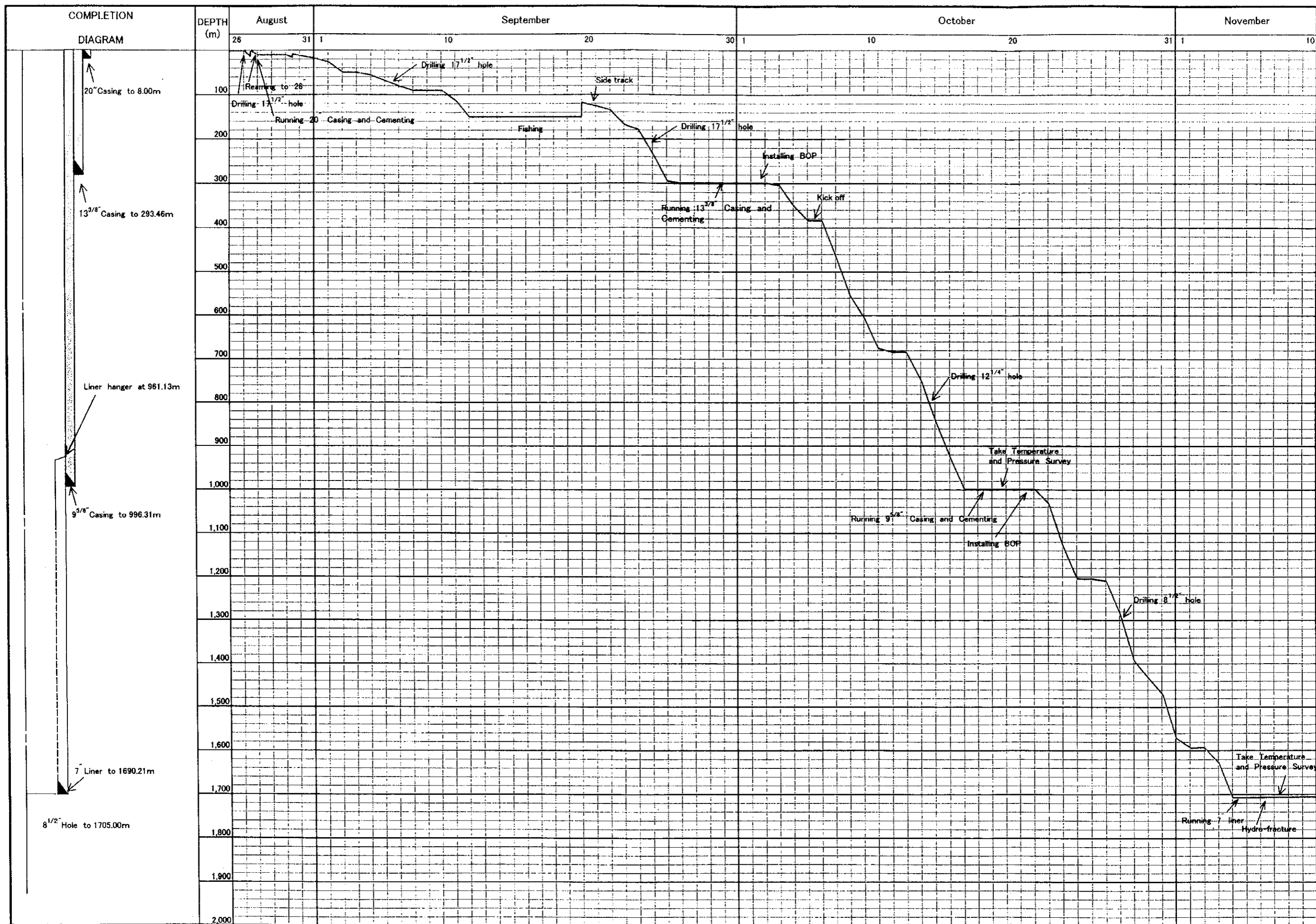


Fig. 2-3-4 AMJ-2 Well Drilling Diagram

AMJ-2号井 掘削実績

